Chapter 5
Gyroscopic Control in Self-Guidance Systems of Flying Objects

In this chapter a gyroscopic control in self-guidance systems of flying objects (FOs) is presented, and a gyroscopic control in an unmanned aerial vehicle is studied. First, the navigational kinematics of an unmanned aerial vehicle (UAV) is analyzed, and then the control of a gyroscope fixed on its board as well as its full control are discussed. Furthermore, a gyroscope in a guided aerial bomb is studied. It includes analysis of kinematics of a bomb self-guided motion to a ground target, equations of motion of a guided bomb, and a description of a gyroscopic system designed for bomb control including automatic pilot control.

5.1 Gyroscope in an Unmanned Aerial Vehicle

The functioning of a UAV at every stage of its operation is a complicated process that requires a complex of technical tasks. The basis of this is the UAV control system. In the course of a mission, there occurs, firstly, the measurement, evaluation, and checking of flight parameters and technical systems, and, secondly, the appropriate control of the flight, system observation, and laser illumination conducted according to the results of identification and checking of the aforementioned parameters. Both the identification and checking, as well as the control, are realized either directly by the operator or automatically.

A fundamental drawback of UAV functioning is the need to maintain two-way communications (often continuously) with a ground control post, which may disclose the post's location, although a variety of means is used to hide the communications. That is why in modern UAV systems autonomy during the realisation of the task of seeking and tracking a ground target is of the utmost importance. It is required that during a programmed flight of a UAV, there must be a way to adjust or even completely change the flight path, depending on the situation, for instance, after target detection.

Modern so-called precision weapons, such as missiles, rockets, and bombs (MRBs), controlled by semiactive self-guidance to a target, find a wide range of

J. Awrejcewicz and Z. Koruba, *Classical Mechanics*, Advances in Mechanics and Mathematics 30, DOI 10.1007/978-1-4614-3978-3_5,

applications. Semiactive methods of MRB path control require so-called target illumination, which is realized by means of a radar beam or rays in the infrared band. The latter are exploited ever more often because of their well-known advantages.

Target illumination is usually conducted from ground stations or from the air, from airplanes and helicopters. This kind of target illumination has many disadvantages. Illumination requires exposing a target. In the case of illumination from ground stations, the target can be covered by natural obstacles. Moreover, the station can be easily detected and destroyed by the enemy. With illumination from the air, manned airplanes or helicopters are used. The need for illumination for a limited amount of time exposes the aerial vehicles to possible danger. Those drawbacks are largely mitigated if a small UAV is used for illumination. If produced using "stealth" technology, given its small dimensions, it is less likely to be detected and shot down. The control problem then becomes illuminating targets with sufficient accuracy.

On the modern battlefield, light, small UAVs produced using stealth technology, which makes them difficult to detect and shoot down, are used for the detection, tracking, and laser illumination of ground targets. A further development of these vehicles is the combat UAV, whose task is the autonomous detection and destruction of targets. An example of this is the use of onboard homing missiles with infrared sensors (trials have been made with a combat version of the Israeli Pioneer [1, 2]. Another example is a UAV equipped with a warhead that can automatically direct itself toward a target according to a defined guidance algorithm (e.g., the American Lark [3]). In this research, a control algorithm for this kind of combat UAV independently attacking detected targets (e.g., radar stations, combat vehicles, tanks) or conducting illumination using a laser has been proposed (Fig. 5.1).

5.1.1 Navigation Kinematics of a UAV

Figure 5.2 schematically depicts the geometric relationships of the kinematics of relative motion of particles S and C (mass centers of UAV and target) and G (point of intersection of a target seeking and observation line—the TSOL—with Earth's surface).

Based on this and the following figures (Figs. 5.3 and 5.4), the equations of the kinematics of motion of a UAV, TSOL, point G, and a target are derived.

5.1.1.1 Kinematic Equations of UAV Motion

The relative position of axes of the Earth-fixed coordinate system $O_o x'_o y'_o z'_o$ and the system associated with position vector $\mathbf{R}_{es}$ (joining points O_o and S) $O_o x_{es} y_{es} z_{es}$ is defined by two angles φ^s_χ and φ^s_γ.

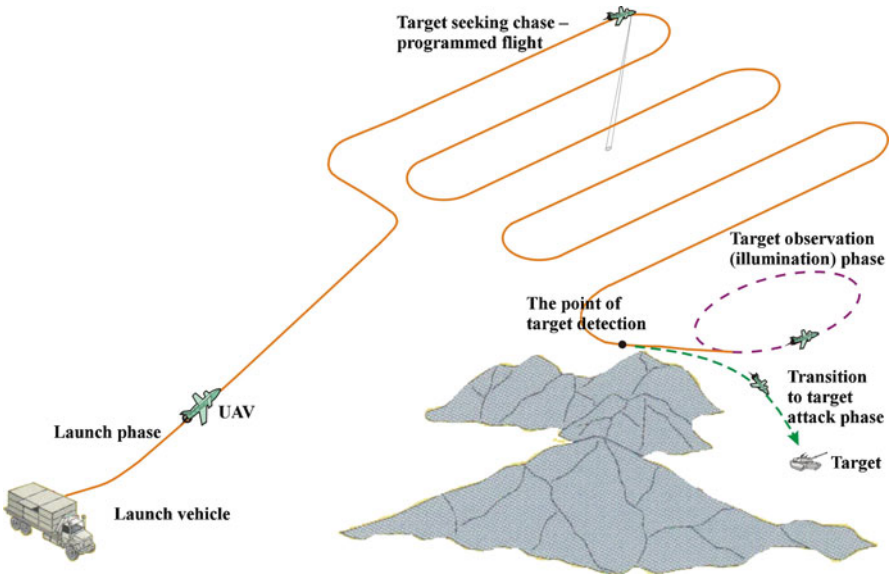

Fig. 5.1 Overall view of process of mission realization by a combat UAV

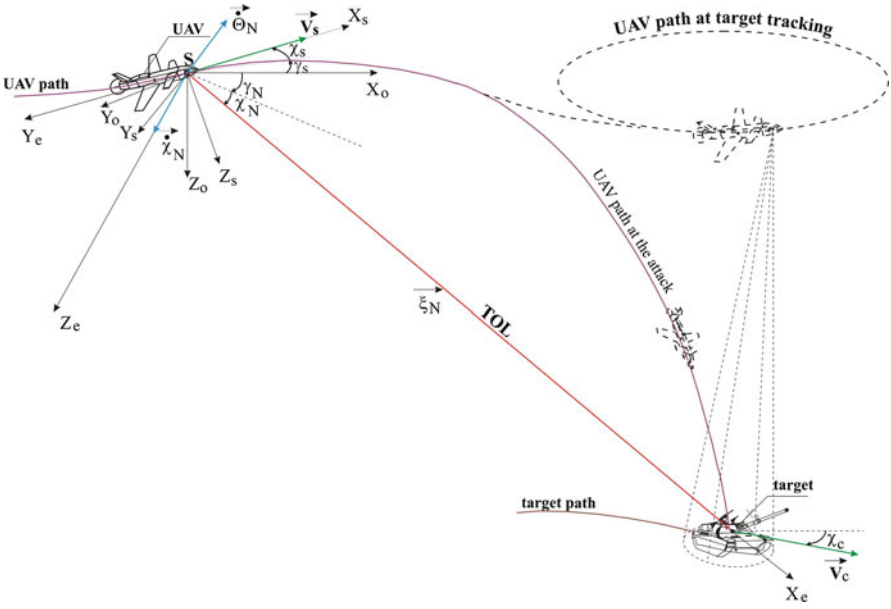

Fig. 5.2 Kinematics of a combat UAV guidance to a moving target

The relative angular positions of the axes of the coordinate systems are defined by direction cosines given in the form of tables or matrices. We obtain the following tables of direction cosines (transformation matrices).

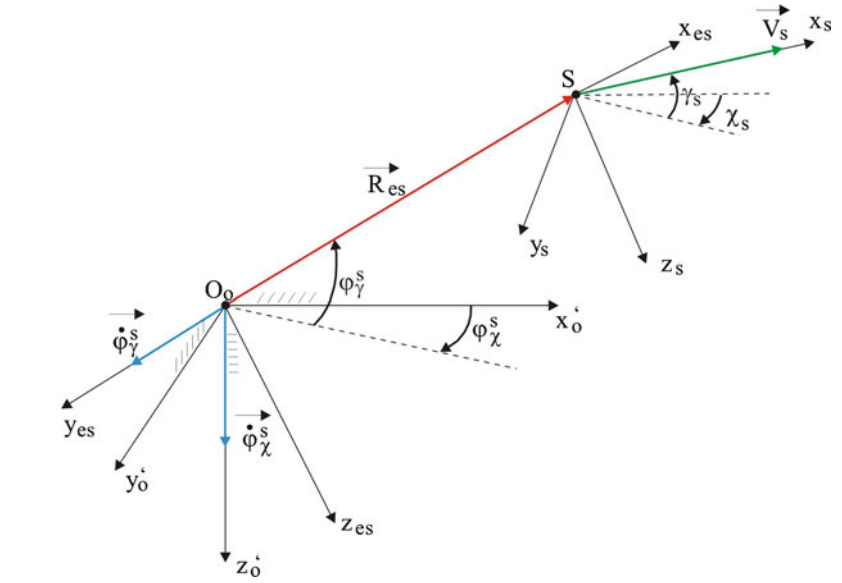

Fig. 5.3 Kinematics of UAV motion

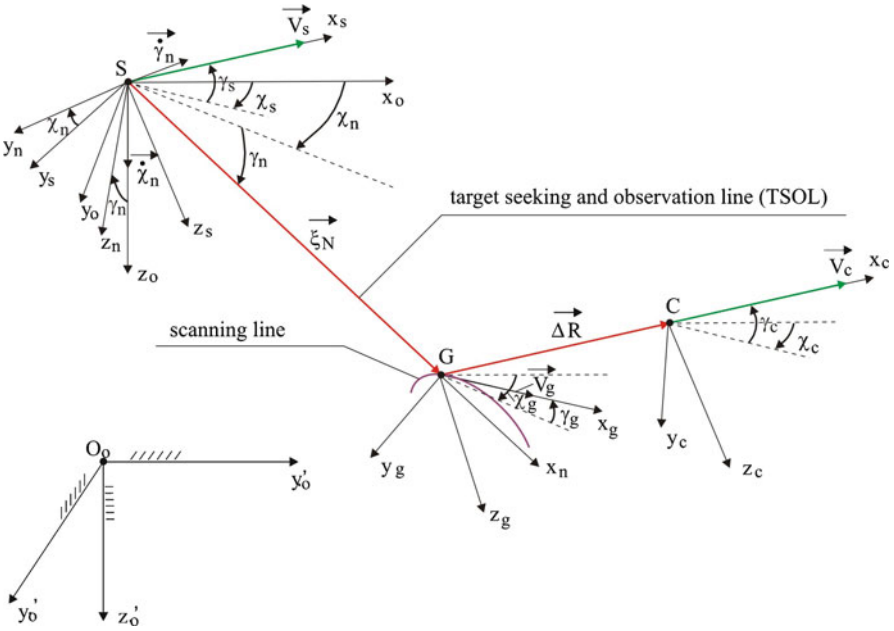

Fig. 5.4 Kinematics of TSOL line motion

The matrix of transformation from the stationary Earth-fixed coordinate system $O_o x'_o y'_o z'_o$ to the instantaneous coordinate system $O_o x_\chi y_\chi z_\chi$ (after the first rotation about the axis $O_o z_o$) is as follows:

$$M_\chi = \begin{array}{c|ccc} & x_o & y_o & z_o \\ \hline x_\chi & \cos\varphi^s_\chi & \sin\varphi^s_\chi & 0 \\ y_\chi & -\sin\varphi^s_\chi & \cos\varphi^s_\chi & 0 \\ z_\chi & 0 & 0 & 1 \end{array}$$

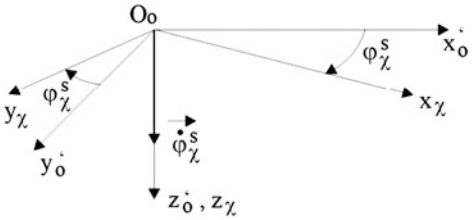

The matrix of transformation from the system $O_o x_\chi y_\chi z_\chi$ to the system $O_o x_{es} y_{es} z_{es}$ (after the second rotation about the instantaneous axis of rotation $O_o y_\chi$) is

$$M_\gamma = \begin{array}{c|ccc} & x_\chi & y_\chi & z_\chi \\ \hline x_{es} & \cos\varphi^s_\gamma & 0 & -\sin\varphi^s_\gamma \\ y_{es} & 0 & 1 & 0 \\ z_{es} & \sin\varphi^s_\gamma & 0 & \cos\varphi^s_\gamma \end{array}$$

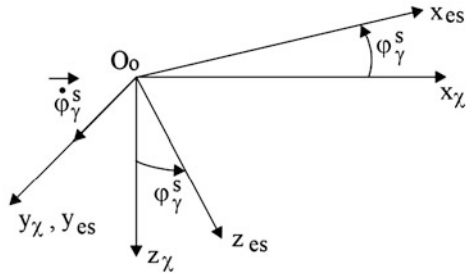

The matrix of transformation from the Earth-fixed coordinate system $O_o x_o y_o z_o$ to the system $O_o x_{es} y_{es} z_{es}$ is as follows:

$$M_{\chi\gamma} = M_\chi \cdot M_\gamma = \begin{bmatrix} \cos\varphi^s_\gamma \cos\varphi^s_\chi & \cos\varphi^s_\gamma \sin\varphi^s_\chi & -\sin\varphi^s_\gamma \\ -\sin\varphi^s_\chi & \cos\varphi^s_\chi & 0 \\ \sin\varphi^s_\gamma \cos\varphi^s_\chi & \sin\varphi^s_\gamma \sin\varphi^s_\chi & \cos\varphi^s_\gamma \end{bmatrix}. \tag{5.1}$$

Proceeding in an analogous way we obtain the matrix of transformation from the Earth-fixed coordinate system $O_o x_o y_o z_o$ to the system associated with the velocity vector of the UAV $S x_s y_s z_s$, i.e.,

$$M^s_{\chi\gamma} = \begin{bmatrix} \cos\gamma_s \cos\chi_s & \cos\gamma_s \sin\chi_\chi & -\sin\gamma_s \\ -\sin\chi_s & \cos\chi_s & 0 \\ \sin\gamma_s \cos\chi_s & \sin\gamma_s \sin\chi_s & \cos\gamma_s \end{bmatrix}. \tag{5.2}$$

The time derivative of vector $\mathbf{R}_{es}$ is equal to the vector of flight velocity $\mathbf{V}_s$ of the UAV, namely,

$$\frac{\mathrm{d}\mathbf{R}_{es}}{\mathrm{d}t} = \mathbf{V}_s. \tag{5.3}$$

Let us project the preceding vector equation onto the axes of the coordinate system $O_o x_{es} y_{es} z_{es}$:

$$\frac{\mathrm{d}\mathbf{R}_{es}}{\mathrm{d}t} = \mathbf{i}_{es}\frac{\mathrm{d}R_{es}}{\mathrm{d}t} + \boldsymbol{\omega}_{es} \times \mathbf{R}_{es} = \mathbf{i}_{es}\frac{\mathrm{d}R_{es}}{\mathrm{d}t} + \begin{vmatrix} \mathbf{i}_{es} & \mathbf{j}_{es} & \mathbf{k}_{es} \\ \omega_{xes} & \omega_{yes} & \omega_{zes} \\ R_{es} & 0 & 0 \end{vmatrix}$$

$$= \mathbf{i}_{es}\frac{\mathrm{d}R_{es}}{\mathrm{d}t} + \mathbf{j}_{es} R_{es}\omega_{zes} - \mathbf{k}_{es} R_{es}\omega_{yes}. \tag{5.4}$$

Vector $\boldsymbol{\omega}_{es}$ in (5.4) is the vector of angular velocity of vector $\mathbf{R}_{es}$, and it can be represented in the form of the following sum of vectors:

$$\boldsymbol{\omega}_{es} = \dot{\boldsymbol{\varphi}}^s_\chi + \dot{\boldsymbol{\varphi}}^s_\gamma. \tag{5.5}$$

The projections are determined by means of matrix (5.1), and we obtain

$$\begin{bmatrix} \omega_{xes} \\ \omega_{xes} \\ \omega_{xes} \end{bmatrix} = M_{\chi\gamma}\begin{bmatrix} 0 \\ 0 \\ \dot{\varphi}^s_\chi \end{bmatrix} + \begin{bmatrix} 0 \\ \dot{\varphi}^s_\gamma \\ 0 \end{bmatrix}. \tag{5.6}$$

Hence

$$\begin{aligned} \omega_{xes} &= -\dot{\varphi}^s_\chi \sin\varphi^s_\gamma, \\ \omega_{yes} &= -\dot{\varphi}^s_\gamma, \\ \omega_{zes} &= -\dot{\varphi}^s_\chi \cos\varphi^s_\gamma, \end{aligned} \tag{5.7}$$

and by virtue of (5.4) we obtain

$$\left(\frac{\mathrm{d}\mathbf{R}_{es}}{\mathrm{d}t}\right)_{xes} = \frac{\mathrm{d}R_{es}}{\mathrm{d}t}, \quad \left(\frac{\mathrm{d}\mathbf{R}_{es}}{\mathrm{d}t}\right)_{yes} = R_{es}\dot{\varphi}^s_\chi \cos\varphi^s_\gamma, \quad \left(\frac{\mathrm{d}\mathbf{R}_{es}}{\mathrm{d}t}\right)_{zes} = -R_{es}\dot{\varphi}^s_\gamma. \tag{5.8}$$

Similarly, projecting velocity vector $\mathbf{V}_s$ onto the axes $O_o x_{es} y_{es} z_{es}$ we obtain

$$\begin{bmatrix} V_{sxes} \\ V_{syes} \\ V_{szes} \end{bmatrix} = M_{\chi\gamma} \cdot M^{\mathrm{T}}_{\chi\gamma}\begin{bmatrix} V_s \\ 0 \\ 0 \end{bmatrix},$$

or equivalently

$$\begin{aligned} V_{sxes} &= V_s\left[\cos\left(\varphi^s_\chi - \chi_s\right)\cos\varphi^s_\gamma \cos\gamma_s + \sin\varphi^s_\gamma \sin\gamma_s\right], \\ V_{syes} &= -V_s \sin\left(\varphi^s_\chi - \chi_s\right)\cos\gamma_s, \\ V_{szes} &= V_s\left[\cos\left(\varphi^s_\chi - \chi_s\right)\sin\varphi^s_\gamma \cos\gamma_s - \cos\varphi^s_\gamma \sin\gamma_s\right]. \end{aligned} \tag{5.9}$$

Projections of the left- and right-hand sides of (5.3) onto axes of the system $O_o x_{es} y_{es} z_{es}$ give the following system of equations:

$$\frac{\mathrm{d}R_{es}}{\mathrm{d}t} = V_s\left[\cos\left(\varphi_\chi^s - \chi_s\right)\cos\varphi_\gamma^s\cos\gamma_s + \sin\varphi_\gamma^s\sin\gamma_s\right], \quad (5.10a)$$

$$\frac{\mathrm{d}\varphi_\chi^s}{\mathrm{d}t}R_{es}\cos\varphi_\gamma^s = -V_s\sin\left(\varphi_\chi^s - \chi_s\right)\cos\gamma_s, \quad (5.10b)$$

$$\frac{\mathrm{d}\varphi_\gamma^s}{\mathrm{d}t}R_{es} = V_s\left[\cos\left(\varphi_\chi^s - \chi_s\right)\sin\varphi_\gamma^s\cos\gamma_s - \cos\varphi_\gamma^s\sin\gamma_s\right]. \quad (5.10c)$$

The preceding equations represent the motion of point S (mass center of a UAV) with respect to the stationary point O_o (the origin of the Earth-fixed coordinate system). The path of motion of the UAV in the Earth-fixed coordinate system is described by the following equations:

$$\begin{aligned} x_{sx_0} &= R_{es}\cos\varphi_\gamma^s\cos\varphi_\chi^s, \\ y_{sx_0} &= R_{es}\cos\varphi_\gamma^s\sin\varphi_\chi^s, \\ z_{sz_0} &= -R_{es}\sin\varphi_\gamma^s. \end{aligned} \quad (5.11)$$

5.1.1.2 Equations of Motion of the Target Seeking and Observation Line (TSOL)

Proceeding in an analogous way to the case of the kinematic equations of motion of a UAV we obtain the following equations: of motion of the TSOL:

$$\begin{aligned} \frac{\mathrm{d}\xi_N}{\mathrm{d}t} &= \Pi(t_0, t_w)\cdot(V_{sxn} - V_{gxn}) + [\Pi(t_w, t_s) \\ &\quad + \Pi(t_s, t_k)]\cdot(V_{sxn} - V_{cxn}), \end{aligned} \quad (5.12)$$

$$\begin{aligned} -\frac{\mathrm{d}\chi_n}{\mathrm{d}t}\xi_N\cos\gamma_n &= \Pi(t_0, t_w)\cdot(V_{syn} - V_{gyn}) \\ &\quad + [\Pi(t_w, t_s) + \Pi(t_s, t_k)]\cdot(V_{syn} - V_{cyn}), \end{aligned} \quad (5.13)$$

$$\begin{aligned} \frac{\mathrm{d}\gamma_n}{\mathrm{d}t}\xi_N &= \Pi(t_0, t_w)\cdot(V_{szn} - V_{gzn}) \\ &\quad + [\Pi(t_w, t_s) + \Pi(t_s, t_k)]\cdot(V_{szn} - V_{czn}). \end{aligned} \quad (5.14)$$

Equations (5.12)–(5.14) are distributive equations with respect to the functions of a square impulse $\Pi(\cdot)$. Thus, they offer way to describe the changes in motion of the TSOL in its various phases.

The components of velocity vectors $\mathbf{V}_S$, $\mathbf{V}_G$, and $\mathbf{V}_C$ in the relative coordinate system $Sx_ny_nz_n$ are as follows:

$$V_{sxn} = V_s\left[\cos(\chi_n - \chi_s)\cos\gamma_n\cos\gamma_s - \sin\gamma_n\sin\gamma_s\right], \tag{5.15a}$$

$$V_{syn} = -V_s\sin(\chi_n - \chi_s)\cos\gamma_s, \tag{5.15b}$$

$$V_{szn} = V_s\left[\cos(\chi_n - \chi_s)\sin\gamma_n\cos\gamma_s - \cos\gamma_n\sin\gamma_s\right], \tag{5.15c}$$

$$V_{gxn} = V_g\left(\cos(\chi_n - \chi_g)\cos\gamma_n\cos\gamma_g - \sin\gamma_n\sin\gamma_g\right), \tag{5.16a}$$

$$V_{gyn} = -V_g\sin(\chi_n - \chi_g)\cos\gamma_g, \tag{5.16b}$$

$$V_{gzn} = V_g\left(\cos(\chi_n - \chi_g)\sin\gamma_n\cos\gamma_g - \cos\gamma_n\sin\gamma_g\right), \tag{5.16c}$$

$$V_{cxn} = V_c\left[\cos(\chi_n - \chi_c)\cos\gamma_n\cos\gamma_c - \sin\gamma_n\sin\gamma_c\right], \tag{5.17a}$$

$$V_{cyn} = -V_c\sin(\chi_n - \chi_c)\cos\gamma_c, \tag{5.17b}$$

$$V_{czn} = V_c\left[\cos(\chi_n - \chi_c)\sin\gamma_n\cos\gamma_c - \cos\gamma_n\sin\gamma_c\right]. \tag{5.17c}$$

5.1.1.3 Path of Motion of Point *G*

This motion is governed by the following equations (Fig. 5.5):

$$\begin{aligned}\frac{\mathrm{d}R_{eg}}{\mathrm{d}t} &= \Pi(t_0,t_w)V_g\cos\left(\varphi_g - \chi_g\right),\\ \frac{\mathrm{d}\varphi_g}{\mathrm{d}t} &= \Pi(t_0,t_w)V_g\sin\left(\varphi_g - \chi_g\right),\end{aligned} \tag{5.18a}$$

$$\begin{aligned}x_{gx_0} &= R_{eg}\cos\varphi_g,\\ y_{gy_0} &= R_{eg}\sin\varphi_g.\end{aligned} \tag{5.18b}$$

5.1.1.4 Kinematics of Motion of a Target

Proceeding in an analogous way to the case of the derivation of kinematic equations of motion of a UAV and using Fig. 5.4, we obtain the following equations of motion of a target (Fig. 5.6):

$$\frac{\mathrm{d}R_{ec}}{\mathrm{d}t} = V_c\left[\cos\left(\varphi_\chi^c - \chi_c\right)\cos\varphi_\gamma^c\cos\gamma_c + \sin\varphi_\gamma^c\sin\gamma_c\right], \tag{5.19a}$$

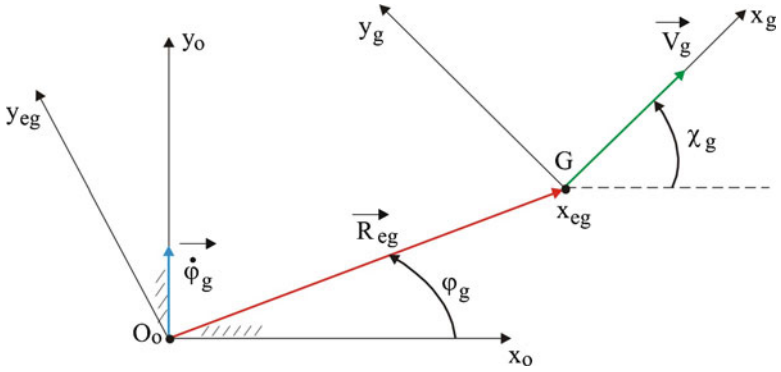

Fig. 5.5 Kinematics of motion of the point *G*

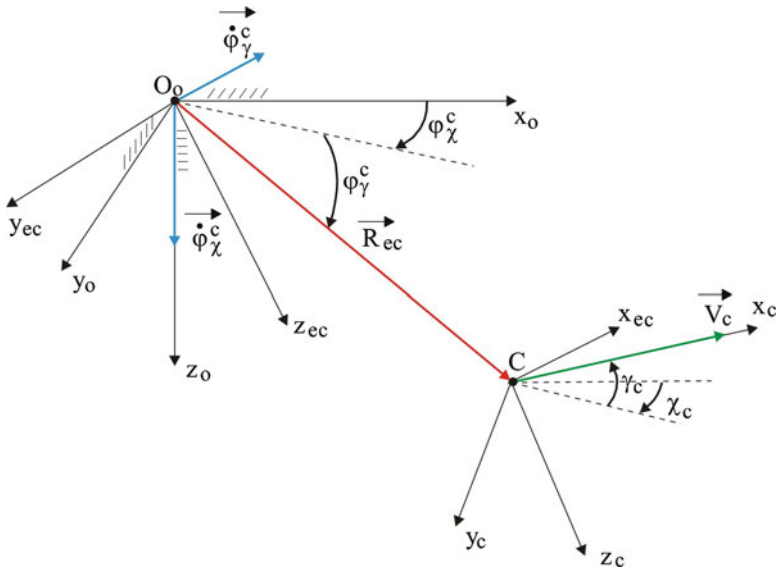

Fig. 5.6 Kinematics of target motion

$$\frac{\mathrm{d}\varphi_{\chi}^{c}}{\mathrm{d}t} R_{ec} \cos\varphi_{\gamma}^{c} = -V_c \sin\left(\varphi_{\chi}^{c} - \chi_s\right) \cos\gamma_c, \tag{5.19b}$$

$$\frac{\mathrm{d}\varphi_{\gamma}^{c}}{\mathrm{d}t} R_{ec} = V_c \left[\cos\left(\varphi_{\chi}^{c} - \chi_c\right) \sin\varphi_{\gamma}^{c} \cos\gamma_c - \cos\varphi_{\gamma}^{c} \sin\gamma_c\right]. \tag{5.19c}$$

A path of target motion in an Earth-fixed coordinate system is described by the equations

$$x_{cx_0} = R_{ec} \cos\varphi_{\gamma}^{c} \cos\varphi_{\chi}^{c},$$

$$\begin{aligned} y_{sx_0} &= R_{ec} \cos \varphi_\gamma^c \sin \varphi_\chi^c, \\ z_{sz_0} &= -R_{ec} \sin \varphi_\gamma^c. \end{aligned} \tag{5.20}$$

Determining desired angles of flight of a UAV

The angles of flight χ_s and γ_s of a UAV seeking and attacking a detected target are determined from the following relationships:

$$\chi_s^* = \Pi\left(t_o, t_w\right) \cdot \chi_s^p + \Pi\left(t_w, t_k\right) \cdot \chi_s^n, \tag{5.21}$$

$$\gamma_s^* = \Pi\left(t_o, t_w\right) \cdot \gamma_s^p + \Pi\left(t_w, t_k\right) \cdot \gamma_s^n. \tag{5.22}$$

The functions of square impulse $\Pi(\cdot)$ offer a method for describing the changes in angles of UAV flight in various phases.

In turn, the angles of flight of the UAV χ_s and γ_s during seeking, the transition to a tracking phase, and laser illumination of a detected target are as follows:

$$\chi_s^* = \Pi\left(t_o, t_w\right) \cdot \chi_s^p + \Pi\left(t_w, t_s\right) \cdot \chi_s^t + \Pi\left(t_s, t_k\right) \cdot \chi_s^o, \tag{5.23}$$

$$\gamma_s^* = \Pi\left(t_o, t_w\right) \cdot \gamma_s^p + \Pi\left(t_w, t_s\right) \cdot \gamma_s^t + \Pi\left(t_s, t_k\right) \cdot \gamma_s^o. \tag{5.24}$$

The quantities χ_s^p and γ_s^p denote the programmed angles of flight of a UAV while patrolling the Earth's surface (target seeking), and they are the prescribed time functions

$$\chi_s^p = \chi_s^p\left(t\right), \qquad \gamma_s^p = \gamma_s^p\left(t\right). \tag{5.25}$$

Before determining a UAV's flight angles χ_s^o and γ_s^o for the case of tracking and simultaneous laser illumination of a detected target, let us introduce the following assumptions [4–6].

For the sake of simplification of calculation, let us assume that UAV motion, both during penetration and tracking, takes place in a horizontal plane at a given altitude H_S, whereas the target and point G move in the Earth's plane. Then we can assume that

$$\gamma_s^o = 0, \qquad \gamma_c = 0, \qquad \gamma_g = 0. \tag{5.26}$$

Let us additionally introduce, for the convenience of notation, the following symbol:

$$r_N = \xi_N \cos \gamma_n \tag{5.27}$$

and calculate the time derivative of this expression:

$$\frac{\mathrm{d}r_N}{\mathrm{d}t} = \frac{\mathrm{d}\xi_N}{\mathrm{d}t} \cos \gamma_n - \xi_N \frac{\mathrm{d}\gamma_n}{\mathrm{d}t} \sin \gamma_n. \tag{5.28}$$

Taking into account (5.26)–(5.28), we can limit our further calculations to plane motion in the horizontal plane and represent (5.12)–(5.14), after the substitution of (5.26)–(5.28), in the following form:

$$\begin{aligned}\frac{\mathrm{d}r_N}{\mathrm{d}t} &= \Pi(t_0,t_w)\left[V_s\cos\left(\chi_n-\chi_s^p\right)-V_g\cos\left(\chi_n-\chi_g\right)\right]\\ &+\Pi(t_w,t_s)\left[V_s\cos\left(\chi_n-\chi_s^t\right)-V_c\cos\left(\chi_n-\chi_c\right)\right]\\ &+\Pi(t_s,t_k)\left[V_s\cos\left(\chi_n-\chi_s^s\right)-V_c\cos\left(\chi_n-\chi_c\right)\right],\end{aligned} \tag{5.29}$$

$$\begin{aligned}\frac{\mathrm{d}\chi_n}{\mathrm{d}t} &= \Pi(t_0,t_w)\frac{V_s\sin\left(\chi_n-\chi_g\right)-V_g\sin\left(\chi_n-\chi_s^p\right)}{r_N}\\ &+\Pi(t_w,t_s)\cdot\frac{V_s\sin\left(\chi_n-\chi_c\right)-V_c\sin\left(\chi_n-\chi_s^t\right)}{r_N}\\ &+\Pi(t_s,t_k)\frac{V_s\sin\left(\chi_n-\chi_c\right)-V_c\sin\left(\chi_n-\chi_s^s\right)}{r_N}.\end{aligned} \tag{5.30}$$

Let us require that at the instant of target detection the UAV must automatically commence transition to a target tracking flight, which relies on the movement of an aerial vehicle at the constant prescribed distance from the target $r_{N0}=\xi_{N0}\cos\gamma_n=$ const (in the horizontal plane at the constant altitude H_s).

Until the relative distance r_N of points S and C is equal to r_{N0}, the program of change of yaw angle $\chi_s=\chi_s^t$ and $\gamma_s=\gamma_s^t$ are determined from the relationship [7]

$$\frac{\mathrm{d}\chi_s^t}{\mathrm{d}t}=a_\chi\cdot\operatorname{sign}\left(r_{N0}-r_N\right)\frac{\mathrm{d}\chi_n}{\mathrm{d}t},\quad \gamma_s^t=0, \tag{5.31}$$

which results in steering of the UAV so as to approach or depart from the target (depending on the sign of the function $\operatorname{sign}(r_{N0}-r_N)$), according to the so-called proportional navigation method [8–10]. Upon satisfaction of the condition $r_{N0}=r_N$, the program of change of the angle χ_s^o is determined from (5.30), which is transformed into

$$V_s\cos\left(\chi_n-\chi_s^o\right)=V_c\cos\left(\chi_n-\chi_c\right). \tag{5.32}$$

Hence, the flight angles of the UAV during laser illumination of the detected target χ_s^o and γ_s^o, on the assumption that the UAV moves in the horizontal plane at a constant altitude H_s, will be determined from the relationships

$$\chi_s^o=\chi_n-\arccos\left[\frac{V_c}{V_s}\cos(\chi_n-\chi_c)\right],\quad \gamma_s^o=0. \tag{5.33}$$

The flight angles of the UAV while attacking a detected target χ_s^n and γ_s^n will be determined from the relationships describing the proportional navigation method [7, 11]:

$$\frac{\mathrm{d}\chi_s^n}{\mathrm{d}t}=a_\chi\frac{\mathrm{d}\chi_n}{\mathrm{d}t}, \tag{5.34}$$

$$\frac{\mathrm{d}\gamma_s^n}{\mathrm{d}t} = a_\gamma \frac{\mathrm{d}\gamma_n}{\mathrm{d}t}. \tag{5.35}$$

The angles χ_s^* and γ_s^* define the prescribed position of the velocity vector of a missile in space. The difference between the prescribed and actual angular positions of the velocity vector of a UAV is an error, also known as a discrepancy parameter, for a system of automatic control in autopilot. Based on the value and direction of the error, a control signal is elaborated, and after the appropriate transformation, it is transferred to an actuator for displacing control surfaces in a transverse channel and a longitudinal channel by the determined values of the angles.

5.1.2 *Control of an Axis of a Gyroscope on Board a Combat UAV*

It follows from the previous sections that during seeking of a ground target from on-board a UAV, a gyroscope axis should perform required movements, and consequently, because it is being directed downward, it should draw strictly defined lines on the Earth's surface. In this way, the optical system installed in the gyroscope axis, with its angle of view, may encounter a visible light or infrared radiation emitted by a moving apparatus. Thus, the kinematic parameters of relative motion of the gyroscope axis and the UAV board should be selected so that the target can be detected with the highest possible probability. After location of the target (upon reception of the signal by an infrared detector) the gyroscope transitions to a tracking state, that is, from that moment on its axis assumes the specific position in space so as to be directed toward its target.

Control moments M_b, M_c acting on the gyroscope located on board the UAV, will be represented in the following way:

$$M_b = \Pi(t_o, t_w) \cdot M_b^p(t) + \Pi(t_s, t_k) \cdot M_b^s, \tag{5.36}$$

$$M_c = \Pi(t_o, t_w) \cdot M_c^p(t) + \Pi(t_s, t_k) \cdot M_c^s. \tag{5.37}$$

The programmed control moments $M_b^p(t)$ and $M_c^p(t)$ set the gyroscope axis into the required motion and are determined by means of a method for solving the inverse dynamics problem [12, 13]:

$$M_b^p(\tau) = \Pi\,(\tau_0, \tau_w) \cdot \left[\frac{\mathrm{d}^2\vartheta_{gz}}{\mathrm{d}\tau^2} + b_b \frac{\mathrm{d}\vartheta_{gz}}{\mathrm{d}\tau} - \frac{1}{2}\left(\frac{\mathrm{d}\psi_{gz}}{\mathrm{d}\tau}\right)^2 \sin 2\vartheta_{gz} + \right.$$
$$\left. - \frac{\mathrm{d}\psi_{gz}}{\mathrm{d}\tau} \cos\vartheta_{gz} \right] \cdot \frac{1}{c_b}, \tag{5.38}$$

$$M_c^p(\tau) = \Pi(\tau_0, \tau_w) \cdot \left[\frac{\mathrm{d}^2\psi_{gz}}{\mathrm{d}\tau^2} \cos^2\vartheta_{gz}^p + b_c \frac{\mathrm{d}\psi_{gz}}{\mathrm{d}\tau} + \frac{\mathrm{d}\psi_{gz}}{\mathrm{d}\tau} \frac{\mathrm{d}\vartheta_{gz}}{\mathrm{d}\tau} \sin 2\vartheta_{gz} + \frac{\mathrm{d}\vartheta_{gz}}{\mathrm{d}\tau} \cos\vartheta_{gz} \right] \cdot \frac{1}{c_c}, \tag{5.39}$$

where $\tau = t \cdot \Omega$, $\Omega = \frac{J_{go} n_g}{J_{gk}}$, $c_b = c_c = \frac{1}{J_{gk}\Omega^2}$.

The time instant when the target enters a field of view of objective TSOL is equivalent to the following relationship:

$$|\Delta\mathbf{r}| = |\mathbf{r}_c - \mathbf{r}_g| \le \Delta r_{zad}, \tag{5.40}$$

where Δr_{zad} is the prescribed radius of a circle of view of objective TSOL, the control of a gyroscope passes to a tracking state.

If we denote the angular error between the actual angles ϑ_g and ψ_g and the required angles ϑ_{gz} and ψ_{gz} by

$$e_\vartheta = \vartheta_g - \vartheta_{gz}, \tag{5.41a}$$

$$e_\psi = \psi_g - \psi_{gz}, \tag{5.41b}$$

then the control moments of a gyroscope at tracking have the following form:

$$M_b^s(\tau) = \Pi(\tau_s, \tau_k) \cdot \left(\bar{k}_b \cdot e_\vartheta - \bar{k}_c \cdot e_\psi + \bar{h}_g \frac{\mathrm{d}e_\vartheta}{\mathrm{d}\tau} \right), \tag{5.42}$$

$$M_c^s(\tau) = \Pi(\tau_s, \tau_k) \cdot \left(\bar{k}_b \cdot e_\psi + \bar{k}_c \cdot e_\vartheta + \bar{h}_g \frac{\mathrm{d}e_\psi}{\mathrm{d}\tau} \right), \tag{5.43}$$

where $\bar{k}_b = \frac{k_b}{J_{gk}\Omega^2}$, $\bar{k}_c = \frac{k_c}{J_{gk}\Omega^2}$, $\bar{h}_g = \frac{h_g}{J_{gk}\Omega}$. The coefficients k_b, k_c, and h_g are selected in an optimal way using the algorithm presented in [5].

The prescribed angles ϑ_{gz} and ψ_{gz} and their first and second time derivatives occurring in the control laws (5.38), (5.39), (5.42), and (5.43) are determined as presented in [5,9]. If a prismatic scanning device is applied in UWSLOC, the control moments M_b, M_c acting on a gyroscope are as follows:

$$M_b = \Pi(t_o, t_w) \cdot M_b^p(t) + \Pi(t_w, t_z) \cdot M_b^t(t) + \Pi(t_s, t_k) \cdot M_b^s, \tag{5.44a}$$

$$M_c = \Pi(t_o, t_w) \cdot M_c^p(t) + \Pi(t_w, t_z) \cdot M_c^t(t) + \Pi(t_s, t_k) \cdot M_c^s. \tag{5.44b}$$

The additional (as compared to (5.36) and (5.37)) quantities M_b^t and M_c^t that occur in the preceding equations denote the programmed control moments whose task is to move the axis along the shortest path onto the target observation line—the TOL (the line joining points S and C—Fig. 5.4).

Since the moment when the target enters the field of view of a scanning device—the controls of the gyroscope transits to a state where it moves the axis onto the TOL

$$|\Delta\boldsymbol{\rho}^*| = \left|\boldsymbol{\rho}_z^* - \boldsymbol{\rho}_w^*\right| \leq \Delta\rho_{zad}, \tag{5.45}$$

where $\Delta\rho_{zad}$ is the prescribed width of a ring of view of a scanning device.

In order to the determine of the control moments M_b^t and M_c^t that move the gyroscope axis onto the TOL, one should apply the control algorithm described in [10]. Thus, it is necessary to change the moments of forces controlling a gyroscope. It is most convenient at first to require that from the given initial position following detection of the target ϑ_{gz}^w and ψ_{gz}^w the gyroscope axis should be led to the position ϑ_{gz}^* and ψ_{gz}^* by means of $M_b^t = \text{const}$ and $M_c^t = \text{const}$. Thus, we control gyroscope axes in two stages:

1. We act with constant moments $M_b^t = \text{const}$ and $M_c^t = \text{const}$ and after reaching $\vartheta_g = \vartheta_{gz}^*$ and $\psi_g = \psi_{gz}^*$ we proceed to the second stage.
2. We act with moments M_b^s, M_c^s.

Assuming that the target moves at a relatively low speed, that is, $\ddot{\vartheta}_{zo}^w \approx 0$, $\dot{\vartheta}_{gz}^w \approx 0$, $\ddot{\psi}_{gz}^w \approx 0$, $\dot{\psi}_{gz}^w \approx 0$, we obtain the following relationships:

$$\vartheta_g(t) \approx \vartheta_{gz}^w + \frac{\Omega\left(\eta_c M_b^t + M_c^t\right)}{J_{gk}\omega_{go}^2}t, \tag{5.46a}$$

$$\psi_g(\mathrm{t}) \approx \psi_{gz}^w + \frac{\Omega\left(\eta_b M_c^t - M_b^t\right)}{J_{gk}\omega_{go}^2}t, \tag{5.46b}$$

where $\omega_{go}^2 = (1 + \eta_b\eta_c)\cdot\Omega^2$.

The time during which the gyroscope axis is transits from the position ϑ_{gz}^w, ψ_{gz}^w to the position ϑ_{gz}^*, ψ_{gz}^* is equal to the time of maximum prism intensitivity T_w^*. Then, from the preceding equations we obtain

$$\vartheta_{gz}^w + \frac{\Omega\left(\eta_c M_b^t + M_c^t\right)}{J_{gk}\omega_{go}^2}T_w^* = \vartheta_{gz}^*, \tag{5.47a}$$

$$\psi_{gz}^w + \frac{\Omega\left(\eta_b M_c^t - M_b^t\right)}{J_{gk}\omega_{go}^2}T_w^* = \psi_{gz}^*. \tag{5.47b}$$

This is a system of two equations with two unknowns M_b^t and M_c^t. Hence we obtain

$$M_b^t = -\frac{\left(\left(\psi_{gz}^* - \psi_{gz}^w\right) - \left(\vartheta_{gz}^* - \vartheta_{gz}^w\right)\eta_b\right)J_{go}n_g}{T_w^*}, \tag{5.48a}$$

$$M_c^t = \frac{\left(\left(\psi_{gz}^* - \psi_{gz}^w\right)\eta_c + \left(\vartheta_{gz}^* - \vartheta_{gz}^w\right)\right) J_{go} n_g}{T_w^*}. \tag{5.48b}$$

Eventually, for the realization of the gyroscope axis motion intended to obtain alignment with the TOL we apply the following algorithm:

1. For $t_w \le t < T_w^*$ we control with the moments $M_b = M_b^t$ and $M_c = M_c^t$.
2. For $T_w^* \ge t \ge t_k$ we control with the moments $M_b = M_b^s$ and $M_c = M_c^s$.

If in this case we denote the angular errors between the actual angles ϑ_g and ψ_g and the required angles ϑ_{gz}^* and ψ_{gz}^* by

$$e_\vartheta = \vartheta_g - \vartheta_{gz}^*, \qquad e_\psi = \psi_g - \psi_{gz}^*, \tag{5.49}$$

then we write the control moments of the gyroscope at tracking in the form of a law described by (5.42) and (5.43).

The presented mathematical model of the operation of a scanning device installed on board a UAV allows us to conduct numerical investigations of seeking, locating, and tracking of a mobile target (a ground or water one) emitting the infrared radiation.

5.1.3 Control of UAV Motion

The control of UAV motion takes place by means of displacement of control surfaces of ailerons, a rudder, and an elevator respectively by angles δ_l, δ_m, and δ_n.

The realization of a required flight path of the UAV is effected by an automatic pilot (AP), which elaborates control signals for the actuating system of the control based on the derived relationships (5.21)–(5.24).

The control law for the autopilot, including the dynamics of displacement of the rudder and elevator, is described in the following way:

$$\frac{\mathrm{d}^2\delta_m}{\mathrm{d}t^2} + h_{ms}\frac{\mathrm{d}\delta_m}{\mathrm{d}t} + k_{ms}\delta_m = k_m\left(\gamma_s - \gamma_s^*\right) + h_m\left(\frac{\mathrm{d}\gamma_s}{\mathrm{d}t} - \frac{\mathrm{d}\gamma_s^*}{\mathrm{d}t}\right) + b_m \cdot u_m, \tag{5.50}$$

$$\frac{\mathrm{d}^2\delta_n}{\mathrm{d}t^2} + h_{ns}\frac{\mathrm{d}\delta_n}{\mathrm{d}t} + k_{ns}\delta_n = k_n\left(\chi_s - \chi_s^*\right) + h_m\left(\frac{\mathrm{d}\chi_s}{\mathrm{d}t} - \frac{\mathrm{d}\chi_s^*}{\mathrm{d}t}\right) + b_n \cdot u_n. \tag{5.51}$$

Quantities u_m and u_n occurring in the preceding equations denote stabilizing controls elaborated by the automatic control system AP. The rule for the elaboration of the stabilizing controls is presented in [14].

In the course of a mission, a light UAV can be affected by various kinds of disturbances such as wind blasts, vertical ascending and descending motions of air masses, or shockwaves from missiles exploding in the vicinity. At the instant when the target is detected, the UAV automatically transits from its flight along

the programmed trajectory to a flight tracking the target according to the assumed algorithm, in the considered case, maintaining a constant distance from the target. In this way the best conditions are ensured for maintaining the target in the field of view of the objective of a tracking system. A rapid switching of the control system (from one flight stage to the other) can be the cause of disturbance effects of UAV motion dynamics. In turn, the dynamic effects that are the result of the aforementioned disturbances and control switching produce changes in the flight state and the aerodynamic characteristics of the airplane. The time history of maneuvers necessary for the realization of the posed task indicates the existence of distinctly non-linear characteristics of the controlled apparatus [5, 6, 14]. Therefore, for a UAV one should apply the autopilot such that it would be able to provide the assumed accuracy of realization of the programmed and tracking flight while simultaneously ensuring its stability.

5.1.4 Final Remarks

The presented model of navigation and control of a UAV describes the fully autonomous motion of a combat apparatus whose task is not only the detection and identification of a ground target but also its laser illumination or direct attack. The intervention of an operator in the UAV steering can be reduced only to cases where the apparatus is completely diverted off the prescribed course or the target is lost from the field of view of the tracking system's objective (due to wind, missiles, etc.). Thus, there should be a way to automatically send information about such events, and the operator should have the option of taking over the UAV flight control. In further research, both theoretically computational and simulative-experimental, it would be recommended to

(a) Determine the optimal program of a UAV flight.
(b) Elaborate an algorithm for scanning the Earth's surface to provide the quickest detection of targets.
(c) Elaborate a program of time-minimum transition of a UAV from programmed flight to target tracking flight or to self-guidance to a detected target according to the prescribed algorithm.

5.2 Gyroscope in a Guided Aerial Bomb

One characteristic of a bomb attack is that the target is most often known in the form of an image. Even if it emits electromagnetic waves or infrared radiation, the waves or radiation would possess such a small intensity as to be virtually useless. Thus, the target of a bomb attack should be satisfactorily illuminated. Current solutions of guided bombs can be divided into three main groups: bombs requiring marking

of the target by illumination using a laser beam emitted from a separate device, bombs having their own target illumination system, and bombs guided to targets with the aid of a navigation satellite system like a GPS. Within all those groups a fundamental problem is the reliable and accurate guidance of the bomb to the target along an optimal trajectory with respect to time and curvature and at the appropriate angle. A device that is capable of satisfying these requirements would likely be a controlled gyroscope whose axis was a target observation line for a bomb's self-guidance system. It should be emphasized that a gyroscope is not vulnerable to disturbances, and in emergency situations it can replace a GPS system.

Just before a bomb drops from a carrier, the axis of a controlled gyroscope is being directed to the target. From that moment on it represents a target observation line (TOL) that for the bomb's autopilot is the reference for realization of the assumed guidance algorithm (Fig. 5.1). The controlled gyroscope can also be applied in a bomb's television-based guidance system to a ground target. An image of the target's surroundings is transmitted telemetrically or by means of a cable with a bundle of optical fibers to a display being viewed by the operator. With the aid of the display the operator indicates the attack target, that is, he or she appropriately directs the gyroscope axis. From that point the bomb can be steered automatically according to a preset guidance algorithm.

An example of a classic gyroscope suspended on a Cardan joint is the operational unit of a TOL's position control in a target coordinator of a self-guided aerial bomb. Along the gyroscope axis there is installed an optical system of a target-seeking and tracking head. Thus, the accuracy of guidance depends largely on the gyroscope correction system whose task is the minimization of the error between the prescribed motion determined on the fly by the image analysis system and the actual motion. Gyroscope errors are caused mainly by the existence of friction in suspension bearings and non-coincidence of the mass center of the gyroscope's rotor with the point of intersection of suspension frames. For this reason the gyroscope reacts to the kinematic excitation of the base on which it is mounted, that is, to angular motions and changes in the linear velocity of an aerial bomb.

Particularly large changes in the flight parameters of a bomb take place in the initial stage of the guidance process, that is, after the bomb is detached from the carrier and the bomb's native control system is activated. The TOL according to which the bomb guides itself to the target is then determined improperly. With the appearance of excessive deviations of the gyroscope axis from the prescribed orientation, the target's image may be lost from the field of view.

Therefore, a correction system and the parameters of the gyroscope itself should be selected in an optimal way so as to minimize the influence of vibrations of the base (the board of an aerial bomb) on the accuracy of orientation of the gyroscope axis. In this study it was achieved using linear-quadratic regulation (optimization) LQR [15–17].

It is assumed that FO moves ideally along a computed path determined on the basis of the motion of the gyroscope axis. The gyroscope axis, in turn, is controlled in such a way as to obtain its coincidence with the TOL during the self-guidance process.

5.2.1 Kinematics of a Bomb's Self-Guided Motion to a Ground Target

Let us write the equations of motion of a TOL as follows:

$$\frac{\mathrm{d}r_b}{\mathrm{d}t} = V_c\left[\cos(\varepsilon-\gamma_c)\cos\sigma\cos\chi_c+\sin\sigma\sin\chi_c\right] - V_b\left[\cos(\varepsilon-\gamma_b)\cos\sigma\cos\chi_b+\sin\sigma\sin\chi_b\right], \tag{5.52a}$$

$$\frac{\mathrm{d}\sigma}{\mathrm{d}t} = \frac{V_b\left[\cos(\varepsilon-\gamma_b)\sin\sigma\cos\chi_b-\cos\sigma\sin\chi_b\right]}{r_b} + \frac{-V_c\left[\cos(\varepsilon-\gamma_c)\sin\sigma\cos\chi_c-\cos\sigma\sin\chi_c\right]}{r_b}, \tag{5.52b}$$

$$\frac{\mathrm{d}\varepsilon}{\mathrm{d}t} = \frac{V_b\sin(\varepsilon-\gamma_b)\cos\chi_b - V_c\sin(\varepsilon-\gamma_c)\cos\chi_c}{r_b\cos\sigma}, \tag{5.52c}$$

where r_b is the relative distance of the bomb from the target; σ and ϵ are the yaw angle and pitch angle of the TOL, respectively; V_b and V_c are the velocities of motion of the bomb and the target, respectively; χ_b and γ_b are the bomb's angles of flight; and χ_c and γ_c are the angles of flight of the target.

Let us apply a proportional navigation method [6,7] to the guidance of the bomb to the target:

$$\frac{\mathrm{d}\chi_b}{\mathrm{d}t} = a_\sigma\frac{\mathrm{d}\sigma}{\mathrm{d}t}, \tag{5.53}$$

where a_σ, a_ϵ are the constant coefficients of the proportional navigation.

The initial conditions of a bomb's self-guidance are as follows (Fig. 5.7):

$$r_o = \sqrt{(x_{bo}-x_{co})^2+(y_{bo}-y_{co})^2+(z_{bo}-z_{co})^2}, \tag{5.54a}$$

$$\sigma_o = \arcsin\frac{y_{co}-y_{bo}}{r_o}, \tag{5.54b}$$

$$\varepsilon_o = \arctan\frac{z_{bo}-z_{co}}{x_c-x_b}. \tag{5.54c}$$

Let us consider the possibilities for the self-guidance of a bomb such that the attack on the target at the final stage occurs at prescribed angles to the level. Let us additionally assume that the guidance process takes place in the vertical plane. Equations (5.52a) and (5.53) simplify, then, to the form

$$\frac{\mathrm{d}r}{\mathrm{d}t} = V_c\cos(\varepsilon-\gamma_c) - V_s\cos(\varepsilon-\gamma_b), \tag{5.55a}$$

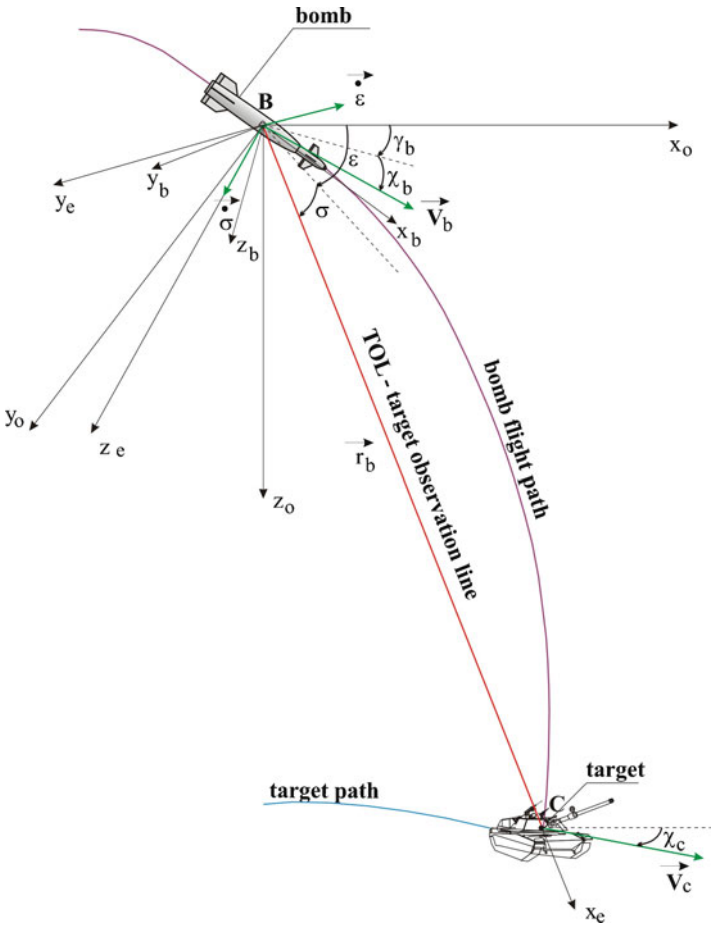

Fig. 5.7 Kinematics of self-guidance of a bomb aimed at a ground target

$$\frac{\mathrm{d}\varepsilon}{\mathrm{d}t} = \frac{V_b \sin(\varepsilon - \gamma_b) - V_c \sin(\varepsilon - \gamma_c)}{r}, \tag{5.55b}$$

$$\frac{\mathrm{d}\gamma_b}{\mathrm{d}t} = a_\varepsilon \frac{\mathrm{d}\varepsilon}{\mathrm{d}t}. \tag{5.55c}$$

Let us move on to the analysis of the kinematics of the self-guidance of a bomb for three special cases of target attack: (1) at an angle of 0° (Fig. 5.8), (2) at an angle of 90° (Fig. 5.9), (3) at an angle of 180° (Fig. 5.10).

Case 1. The attack on a stationary target from a forward hemisphere at an angle of 0°.

Figure 5.8 depicts a possible way to attack a target in the considered case. For this and the two remaining cases, equations of kinematics of motion of a self-guided

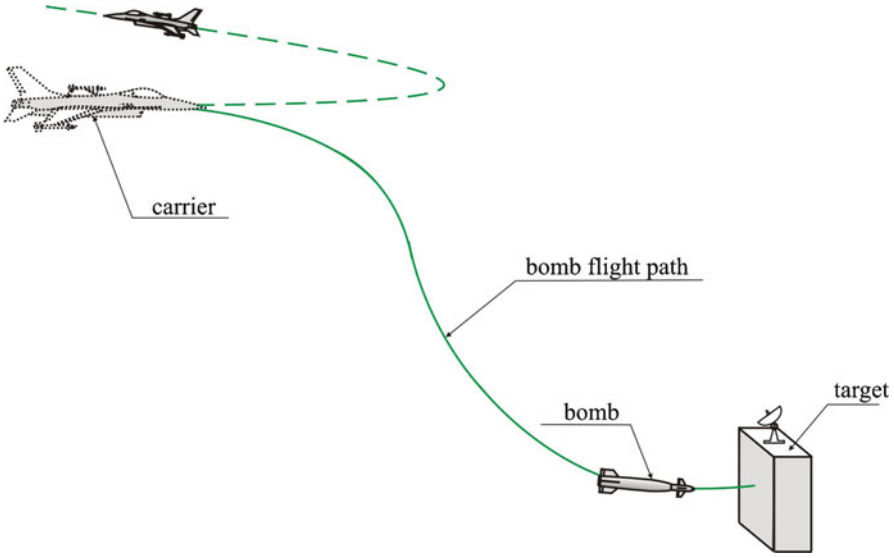

Fig. 5.8 Overall view of self-guidance of a bomb attacking a target at an angle of 0°

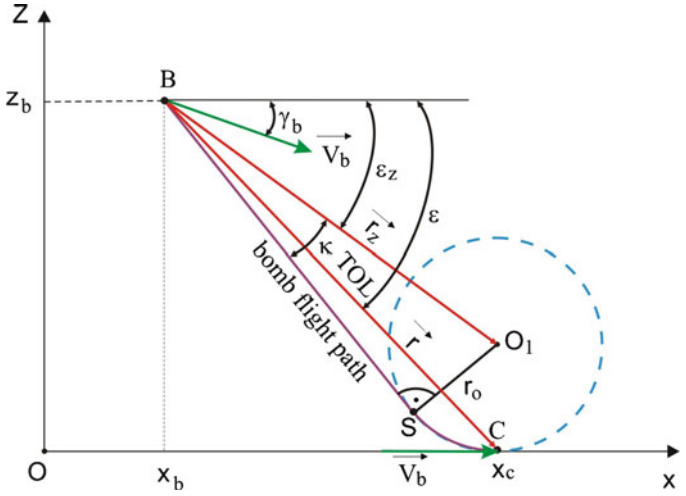

Fig. 5.9 Overall view of self-guidance of a bomb attacking a target at an angle of 90°

bomb will be represented in the following way:

$$\frac{\mathrm{d}r_z}{\mathrm{d}t} = V_c \cos(\varepsilon_z - \gamma_c) - V_b \cos(\varepsilon_z - \gamma_b), \tag{5.56a}$$

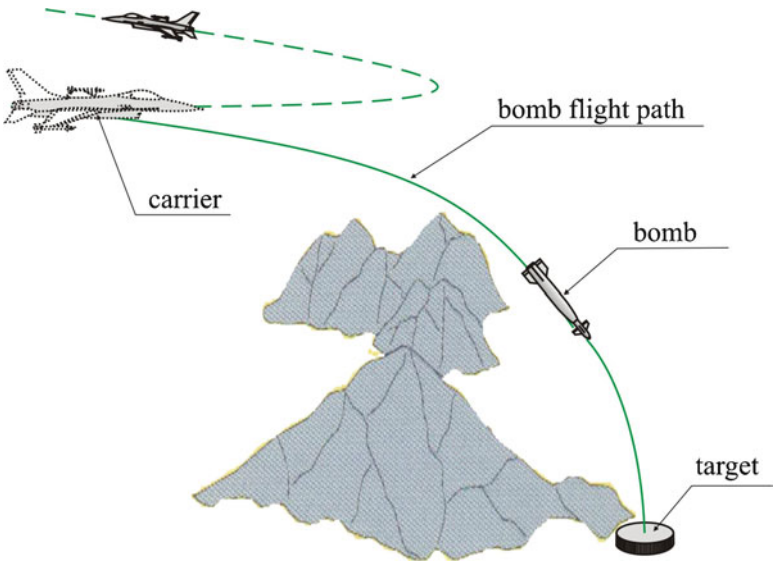

Fig. 5.10 Overall view of self-guidance of a bomb attacking a target at an angle of 180°

$$\frac{\mathrm{d}\varepsilon_z}{\mathrm{d}t} = \frac{V_b \sin(\varepsilon_z - \gamma_b) - V_b \sin(\varepsilon_b - \gamma_c)}{r_z}, \tag{5.56b}$$

$$\frac{\mathrm{d}\gamma_b}{\mathrm{d}t} = a_\gamma \frac{\mathrm{d}\varepsilon^*}{\mathrm{d}t}. \tag{5.56c}$$

According to Fig. 5.11, in which the trigonometric relationships of a bomb's motion are shown, we have

$$\varepsilon^* = \varepsilon_z + \kappa, \qquad \kappa = \arcsin\frac{r_o}{r_z},$$

$$\varepsilon_z = \arctan\frac{z_c - z_b + r_o}{x_c - x_b}, \quad r_z = \sqrt{(z_b - z_c - r_o)^2 + (x_c - x_b)^2},$$

hence

$$\frac{\mathrm{d}\varepsilon^*}{\mathrm{d}t} = \frac{\mathrm{d}\varepsilon_z}{\mathrm{d}t} - \frac{r_o}{\sqrt{r_z^2 - r_o^2}\, r_z}\frac{\mathrm{d}r_z}{\mathrm{d}t}, \tag{5.57}$$

where r_o is the prescribed radius of the circle on whose arc (SC) the bomb moves at the final stage of the flight; r_Z is the distance from point B (mass center of bomb) to the center of the circle that passes through point C (a selected point on the target); κ is the angle between segments BO_1 and BS; and ϵ_z is the "angle of observation" of point O_1.

Case 2. Attacking a stationary target from a forward hemisphere at an angle of 90°.

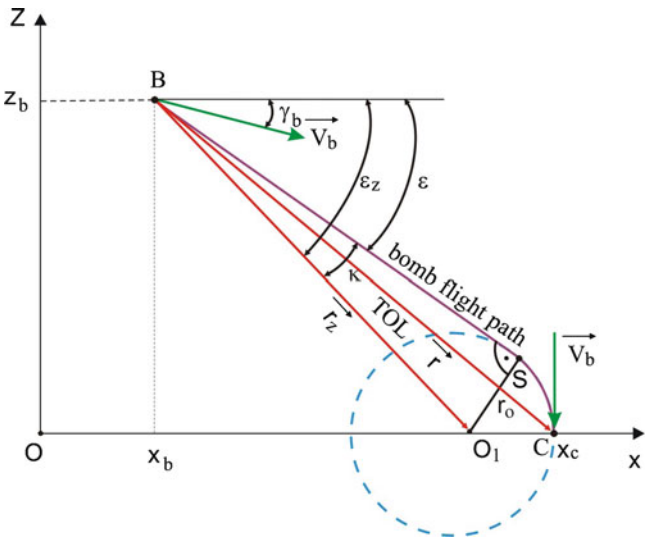

Fig. 5.11 Kinematic schematic of self-guidance of a bomb attacking a target at an angle of 0°

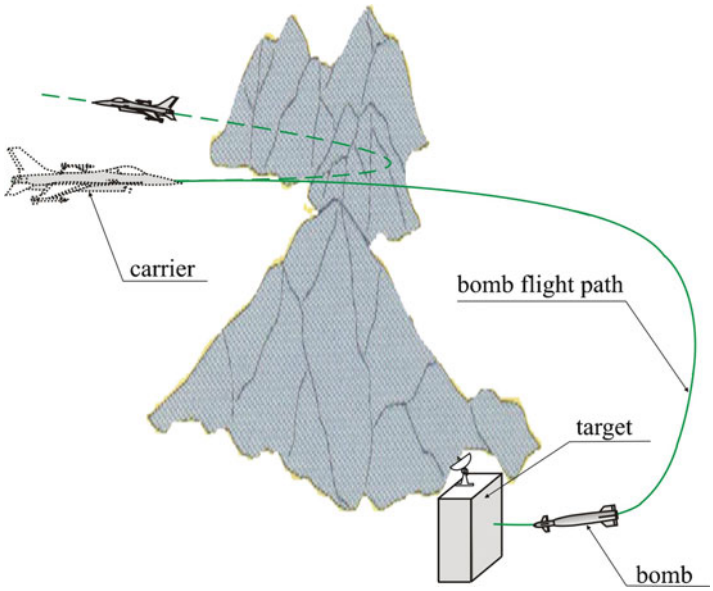

Fig. 5.12 Kinematic schematic of self-guidance of a bomb attacking a target at an angle of 90°

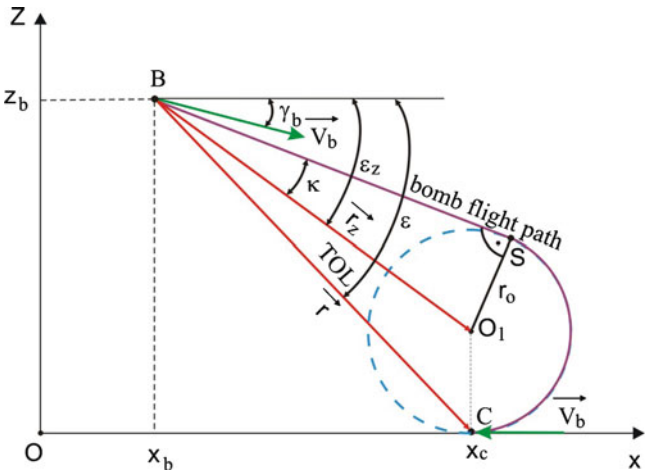

Fig. 5.13 Kinematic schematic of self-guidance of a bomb attacking a target at an angle of 180°

According to Fig. 5.12 we have

$$\varepsilon^* = \varepsilon_z - \kappa, \qquad \kappa = \arcsin\frac{r_o}{r_z},$$

$$\varepsilon_z = \arctan\frac{z_c - z_b}{x_c - x_b - r_o}, \quad r_z = \sqrt{(z_b - z_c)^2 + (x_c - x_b - r_o)^2},$$

hence

$$\frac{\mathrm{d}\varepsilon^*}{\mathrm{d}t} = \frac{\mathrm{d}\varepsilon_z}{\mathrm{d}t} + \frac{r_o}{\sqrt{r_z^2 - r_o^2}\, r_z}\frac{\mathrm{d}r_z}{\mathrm{d}t}. \tag{5.58}$$

Case 3. Attack on a stationary target from a backward hemisphere at an angle of 180°.

According to Fig. 5.13, we have

$$\varepsilon^* = \varepsilon_z - \kappa, \qquad \kappa = \arcsin\frac{r_o}{r_z},$$

$$\varepsilon_z = \arctan\frac{z_c - z_b + r_o}{x_c - x_b}, \quad r_z = \sqrt{(z_b - z_c - r_o)^2 + (x_c - x_b)^2},$$

hence

$$\frac{\mathrm{d}\varepsilon^*}{\mathrm{d}t} = \frac{\mathrm{d}\varepsilon_z}{\mathrm{d}t} + \frac{r_o}{\sqrt{r_z^2 - r_o^2}\, r_z}\frac{\mathrm{d}r_z}{\mathrm{d}t}. \tag{5.59}$$

In all the cases considered previously, at the instant when the bomb reaches point S, that is, at a distance from the target of $r_z = r_o$, it starts moving on a circle of radius $r_o = \text{const}$, and (5.55a) takes the form

$$V_c \cos(\varepsilon_z - \gamma_c) - V_b \cos(\varepsilon_z - \gamma_b) = 0. \tag{5.60}$$

Hence

$$\gamma_b = \varepsilon_z - \arccos\left[\frac{V_c}{V_b}\cos(\varepsilon_z - \gamma_c)\right]. \tag{5.61}$$

In turn, (5.56b) and (5.56c) have the following form:

$$\frac{\mathrm{d}\varepsilon_z}{\mathrm{d}t} = \frac{V_b \sin\left\{\arccos\left[\frac{V_c}{V_b}\cos(\varepsilon_z - \gamma_c)\right]\right\} - V_c \sin(\varepsilon_z - \gamma_c)}{r_o}, \tag{5.62a}$$

$$\frac{\mathrm{d}\gamma_b}{\mathrm{d}t} = \frac{\mathrm{d}\varepsilon_z}{\mathrm{d}t} + \frac{\frac{V_c}{V_b}\left[(\dot{\gamma}_c - \dot{\varepsilon}_z)\sin(\varepsilon_z - \gamma_c) + \left(\frac{\dot{V}_c}{V_c} - \frac{\dot{V}_b}{V_b^2}\right)\cos(\varepsilon_z - \gamma_c)\right]}{\sqrt{1 - \left[\frac{V_c}{V_b}\cos(\varepsilon_z - \gamma_c)\right]^2}}. \tag{5.62b}$$

If the target is stationary ($V_c = 0$), then

$$\gamma_b = \varepsilon_z - \frac{\pi}{2}. \tag{5.63}$$

5.2.2 *Equations of Motion of a Guided Bomb*

We assume that a bomb is a non-deformable (rigid) body of a constant mass. That is why, using Fig. 5.14, the motion of an apparatus can be represented by two systems of equations describing the motion of the mass center of the apparatus and the motion about the mass center [18, 19].

Equations of translational motion

The equations of translational motion of a bomb in its associated coordinate system $O_b xyz$ are as follows:

$$m_b\left(\frac{\mathrm{d}\boldsymbol{u}_b}{\mathrm{d}t} + \boldsymbol{w}_b\boldsymbol{q}_b - \boldsymbol{v}_b\boldsymbol{r}_b\right) - S_x\left(\boldsymbol{q}_b^2 + \boldsymbol{r}_b^2\right) + S_z\left(\frac{\mathrm{d}\boldsymbol{q}_b}{\mathrm{d}t} + \boldsymbol{p}_b\boldsymbol{r}_b\right) = F_x, \tag{5.64a}$$

$$m_b\left(\frac{\mathrm{d}\boldsymbol{v}_b}{\mathrm{d}t} + \boldsymbol{u}_b\boldsymbol{r}_b - \boldsymbol{w}_b\boldsymbol{p}_b\right) + S_x\left(\frac{\mathrm{d}\boldsymbol{r}_b}{\mathrm{d}t} + \boldsymbol{q}_b\boldsymbol{p}_b\right) - S_z\left(\frac{\mathrm{d}\boldsymbol{p}_b}{\mathrm{d}t} - \boldsymbol{q}_b\boldsymbol{r}_b\right) = F_y, \tag{5.64b}$$

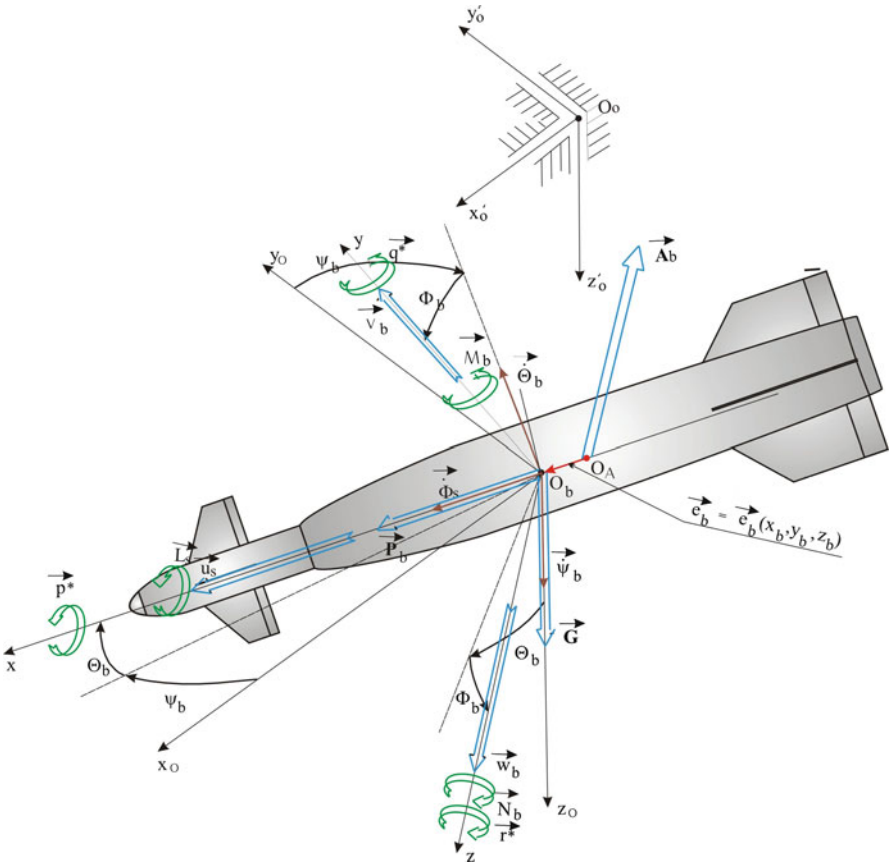

Fig. 5.14 System of forces and moments acting on an FO during flight

$$m_b\left(\frac{\mathrm{d}\boldsymbol{w}_b}{\mathrm{d}t}+\boldsymbol{p}_b\boldsymbol{v}_b-\boldsymbol{q}_b\boldsymbol{u}_b\right)-S_x\left(\frac{\mathrm{d}\boldsymbol{q}_b}{\mathrm{d}t}-\boldsymbol{p}_b\boldsymbol{r}_b\right)-S_z\left(\boldsymbol{q}_b^2+\boldsymbol{p}_b^2\right)=F_z, \quad (5.64c)$$

where

$$\begin{bmatrix}\boldsymbol{F}_x\\ \boldsymbol{F}_y\\ \boldsymbol{F}_z\end{bmatrix}=\begin{bmatrix}\boldsymbol{X}_b+\boldsymbol{G}_x\\ \boldsymbol{Y}_b+\boldsymbol{G}_y\\ \boldsymbol{Z}_b+\boldsymbol{G}_z\end{bmatrix}, \qquad \begin{bmatrix}\boldsymbol{X}_b\\ \boldsymbol{Y}_b\\ \boldsymbol{Z}_b\end{bmatrix}=\frac{d\,(H_b)\,V_b^2}{2}S_b\cdot M_{oz}\cdot\begin{bmatrix}C_x\\ C_y\\ C_z\end{bmatrix}+\begin{bmatrix}\boldsymbol{P}_b\\ 0\\ 0\end{bmatrix},$$

$$V_b=\sqrt{\boldsymbol{u}_b^2+\boldsymbol{v}_b^2+\boldsymbol{w}_b^2},$$

$$M_{oz} = \begin{bmatrix} \cos\Psi_b \cos\Theta_b & \sin\Psi_b \cos\Theta_b & -\sin\Theta_b \\ \sin\varphi_b \cos\Psi_b \sin\Theta_b - \cos\varphi_b \sin\Psi_b & \sin\varphi_b \sin\Psi_b \sin\Theta_b + \cos\varphi_b \cos\Psi_b & \sin\varphi_b \cos\Theta_b \\ \cos\varphi_b \cos\Psi_b \sin\Theta_b + \sin\varphi_b \sin\Psi_b & \cos\varphi_b \sin\Psi_b \sin\Theta_b - \sin\varphi_b \cos\Psi_b & \cos\varphi_b \cos\Theta_b \end{bmatrix},$$

$$\begin{bmatrix} C_x \\ C_y \\ C_z \end{bmatrix} = \begin{bmatrix} C_{xo} \\ C_{yo} \\ C_{zo} \end{bmatrix} + \begin{bmatrix} \frac{\partial C_x}{\partial\alpha} & \frac{\partial C_x}{\partial\beta} & \frac{\partial C_x}{\partial p_s} & \frac{\partial C_x}{\partial q_s} & \frac{\partial C_x}{\partial r_s} & \frac{\partial C_x}{\partial\delta_l} & \frac{\partial C_x}{\partial\delta_m} & \frac{\partial C_x}{\partial\delta_n} & \frac{\partial C_x}{\partial\delta_t} \\ \frac{\partial C_y}{\partial\alpha} & \frac{\partial C_y}{\partial\beta} & \frac{\partial C_y}{\partial p_s} & \frac{\partial C_y}{\partial q_s} & \frac{\partial C_y}{\partial r_s} & \frac{\partial C_y}{\partial\delta_l} & \frac{\partial C_y}{\partial\delta_m} & \frac{\partial C_y}{\partial\delta_n} & \frac{\partial C_y}{\partial\delta_t} \\ \frac{\partial C_z}{\partial\alpha} & \frac{\partial C_z}{\partial\beta} & \frac{\partial C_z}{\partial p_s} & \frac{\partial C_z}{\partial q_s} & \frac{\partial C_z}{\partial r_s} & \frac{\partial C_z}{\partial\delta_l} & \frac{\partial C_z}{\partial\delta_m} & \frac{\partial C_z}{\partial\delta_n} & \frac{\partial C_z}{\partial\delta_t} \end{bmatrix} \cdot \begin{bmatrix} \alpha_b \\ \beta_b \\ \hat{p}_b \\ \hat{q}_b \\ \hat{r}_b \\ \delta_l \\ \delta_m \\ \delta_n \\ \delta_t \end{bmatrix},$$

$$\hat{p}_b = \frac{\boldsymbol{p}_b \cdot b_b}{V_b}, \qquad \hat{q}_b = \frac{\boldsymbol{q}_b \cdot \bar{c}_b}{V_b}, \qquad \hat{r}_b = \frac{\boldsymbol{r}_b \cdot b_b}{V_b}, \qquad \begin{bmatrix} \boldsymbol{G}_x \\ \boldsymbol{G}_y \\ \boldsymbol{G}_z \end{bmatrix} = M_{oz} \cdot \begin{bmatrix} 0 \\ 0 \\ m_b g \end{bmatrix},$$

where m_b is the bomb's mass; $L_b,\ M_b,\ N_b$ are the components of the vector of moment of force acting on the bomb; $u_b,\ v_b,\ w_b$ are the components of the vector of linear velocity of the bomb flight; $p_b,\ q_b,\ r_b$ are the components of the vector of angular velocity of the bomb flight; $F_x,\ F_y,\ F_z$ are the components of the net vector of external forces acting on the bomb; $S_x,\ S_y,\ S_z$ are the static moments with respect to particular axes; $C_x,\ C_y,\ C_z$ are the coefficients of the components of the net aerodynamic force; $d(H_b)$ is the density of the air at a given altitude of bomb flight H_b.

Equations of motion about a point of the FO

Equations of motion about a point of the FO in its associated coordinate system $O_S xyz$ are described by the following system:

$$J_x \frac{\mathrm{d}\boldsymbol{p}_b}{\mathrm{d}t} - (J_y - J_z)\boldsymbol{q}_b \boldsymbol{r}_b - J_{xz}\left(\frac{\mathrm{d}\boldsymbol{r}_b}{\mathrm{d}t} + \boldsymbol{q}_b \boldsymbol{p}_b\right) - S_z\left(\frac{\mathrm{d}\boldsymbol{v}_b}{\mathrm{d}t} - \boldsymbol{w}_b \boldsymbol{p}_b + \boldsymbol{u}_b \boldsymbol{r}_b\right) = \boldsymbol{L}_b, \tag{5.65a}$$

$$J_y \frac{\mathrm{d}\boldsymbol{q}_b}{\mathrm{d}t} - (J_z - J_x)\boldsymbol{r}_b \boldsymbol{p}_b - J_{xz}(\boldsymbol{r}_b^2 - \boldsymbol{p}_b^2) + S_x\left(\frac{\mathrm{d}\boldsymbol{w}_b}{\mathrm{d}t}\boldsymbol{v}_b \boldsymbol{p}_b - \boldsymbol{u}_b \boldsymbol{q}_b\right) + S_z\left(\frac{\mathrm{d}\boldsymbol{u}_b}{\mathrm{d}t} - \boldsymbol{v}_b \boldsymbol{r}_b + \boldsymbol{w}_b \boldsymbol{q}_b\right) = \boldsymbol{M}_b, \tag{5.65b}$$

$$J_z \frac{\mathrm{d}\boldsymbol{r}_b}{\mathrm{d}t} - \left(J_x - J_y\right)\boldsymbol{p}_b \boldsymbol{q}_b - J_{zx}\left(\frac{\mathrm{d}\boldsymbol{p}_b}{\mathrm{d}t} - \boldsymbol{r}_b \boldsymbol{q}_b\right) + S_x\left(\frac{\mathrm{d}\boldsymbol{v}_b}{\mathrm{d}t} - \boldsymbol{w}_b \boldsymbol{p}_b + \boldsymbol{u}_b \boldsymbol{r}_b\right) = \boldsymbol{N}_b, \tag{5.65c}$$

where $J_x,\ J_y,\ J_z$ are the moments of inertia of the bomb with respect to particular axes; $J_{xy},\ J_{yz},\ J_{zx}$ are products of inertia of the bomb.

Furthermore, we have

$$\begin{bmatrix} \boldsymbol{L}_b \\ \boldsymbol{M}_b \\ \boldsymbol{N}_b \end{bmatrix} = \begin{bmatrix} \boldsymbol{L}^A + \boldsymbol{L}_G \\ \boldsymbol{M}^A + \boldsymbol{M}_G \\ \boldsymbol{N}^A + \boldsymbol{N}_G \end{bmatrix}, \qquad \begin{bmatrix} \boldsymbol{L}^A \\ \boldsymbol{M}^A \\ \boldsymbol{N}^A \end{bmatrix} = \frac{d\,(H_b)\,V_b^2}{2} S \cdot M_{oz} \cdot \begin{bmatrix} b_b C_l \\ \bar{c}_b C_m \\ b_b C_n \end{bmatrix},$$

$$\begin{bmatrix} \boldsymbol{L}_G \\ \boldsymbol{M}_G \\ \boldsymbol{N}_G \end{bmatrix} = \begin{bmatrix} m_b g\,(z_b \sin\varphi_b \cos\Theta_b - y_b \cos\varphi_b \cos\Theta_b) \\ m_b g\,(x_b \cos\varphi_b \cos\Theta_b + z_b \sin\Theta_b) \\ -m_b g\,(y_b \sin\Theta_b + x_b \sin\varphi_b \cos\Theta_b) \end{bmatrix},$$

$$\begin{bmatrix} C_l \\ C_m \\ C_n \end{bmatrix} = \begin{bmatrix} C_{lo} \\ C_{mo} \\ C_{no} \end{bmatrix} + \begin{bmatrix} \frac{\partial C_l}{\partial \alpha} & \frac{\partial C_l}{\partial \beta} & \frac{\partial C_l}{\partial p_s} & \frac{\partial C_l}{\partial q_s} & \frac{\partial C_l}{\partial r_s} & \frac{\partial C_l}{\partial \delta_l} & \frac{\partial C_l}{\partial \delta_m} & \frac{\partial C_l}{\partial \delta_n} & \frac{\partial C_l}{\partial \delta_t} \\ \frac{\partial C_m}{\partial \alpha} & \frac{\partial C_m}{\partial \beta} & \frac{\partial C_m}{\partial p_s} & \frac{\partial C_m}{\partial q_s} & \frac{\partial C_m}{\partial r_s} & \frac{\partial C_m}{\partial \delta_l} & \frac{\partial C_m}{\partial \delta_m} & \frac{\partial C_m}{\partial \delta_n} & \frac{\partial C_m}{\partial \delta_t} \\ \frac{\partial C_n}{\partial \alpha} & \frac{\partial C_n}{\partial \beta} & \frac{\partial C_z}{\partial p_s} & \frac{\partial C_n}{\partial q_s} & \frac{\partial C_n}{\partial r_s} & \frac{\partial C_n}{\partial \delta_l} & \frac{\partial C_n}{\partial \delta_m} & \frac{\partial C_n}{\partial \delta_n} & \frac{\partial C_n}{\partial \delta_t} \end{bmatrix} \cdot \begin{bmatrix} \alpha_b \\ \beta_b \\ \hat{p}_b \\ \hat{q}_b \\ \hat{r}_b \\ \delta_l \\ \delta_m \\ \delta_n \\ \delta_t \end{bmatrix},$$

where $C_l,\ C_m,\ C_n$ are the aerodynamic coefficients of a rolling moment L_b, a pitching moment M_b, and a yawing moment N_b, respectively; and g is the acceleration of gravity.

The Kinematic relationships between angular velocities follow

$$\frac{\mathrm{d}\Psi_b}{\mathrm{d}t} = (\boldsymbol{q}_b \sin\varphi_b + \boldsymbol{r}_b \cos\varphi_b)\sec\Theta_b, \tag{5.66a}$$

$$\frac{\mathrm{d}\Theta_b}{\mathrm{d}t} = \boldsymbol{q}_b \cos\varphi_b - \boldsymbol{r}_b \sin\varphi_b, \tag{5.66b}$$

$$\frac{\mathrm{d}\varphi_b}{\mathrm{d}t} = \boldsymbol{p}_b + (\boldsymbol{q}_b \sin\varphi_b + \boldsymbol{r}_b \cos\varphi_b)\tan\Theta_b, \tag{5.66c}$$

where Θ_b, Ψ_b, φ_b are the angles of pitch, yaw, and roll of the longitudinal axis of the bomb, respectively.

The kinematic relationships between linear velocities (a trajectory of a bomb flight) are as follows

$$\begin{aligned}\frac{\mathrm{d}x_o}{\mathrm{d}t} &= \boldsymbol{u}_b \cos\Theta_b \cos\Psi_b + \boldsymbol{v}_b(\sin\varphi_b \sin\Theta_b \cos\Psi_b \\ &\quad - \cos\varphi_b \sin\Psi_b) + \boldsymbol{w}_b\,(\cos\varphi_b \sin\Theta_b \cos\Psi_b + \sin\varphi_b \sin\Psi_b)\,,\end{aligned} \tag{5.67a}$$

$$\begin{aligned}\frac{\mathrm{d}y_o}{\mathrm{d}t} &= \boldsymbol{u}_b \cos\Theta_b \sin\Psi_b + \boldsymbol{v}_b(\sin\varphi_b \sin\Theta_b \sin\Psi_b \\ &\quad + \cos\varphi_b \cos\Psi_b) + \boldsymbol{w}_b\,(\cos\varphi_b \sin\Theta_b \cos\Psi_b + \sin\varphi_b \sin\Psi_b)\,,\end{aligned} \tag{5.67b}$$

$$\frac{\mathrm{d}z_o}{\mathrm{d}t} = -\boldsymbol{u}_b \sin\Theta_b + \boldsymbol{v}_b \sin\varphi_b \cos\Theta_b + \boldsymbol{w}_b \cos\varphi_b \cos\Theta_b, \tag{5.67c}$$

where x_o, y_o, z_o are the coordinates of the center of mass of the bomb in an Earth-fixed coordinate system.

Supplementary relationships are

$$\alpha_b = \arctan\frac{\boldsymbol{w}_b}{\boldsymbol{u}_b}, \tag{5.68a}$$

$$\beta_b = \arcsin\frac{\boldsymbol{v}_b}{\sqrt{\boldsymbol{u}_b^2 + \boldsymbol{v}_b^2 + \boldsymbol{w}_b^2}}, \tag{5.68b}$$

where α_b, β_b are the angles of attack and slip.

5.2.3 A Gyroscopic System of Bomb Control

The task of a gyroscope in a self-guidance system of a bomb can be the determination of a TOL at every time instant. The TOL can be determined in two different

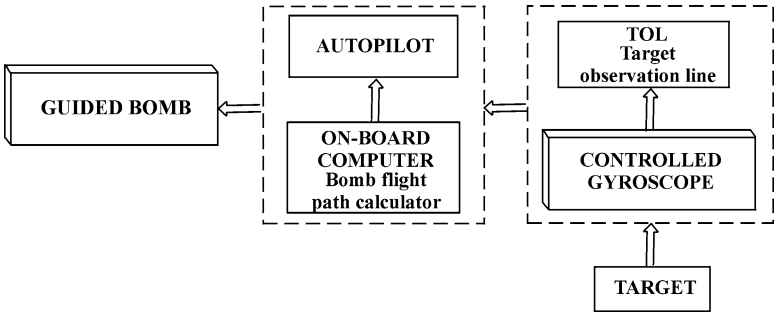

Fig. 5.15 Simplified schematic of bomb self-guidance to a ground target

ways: (1) for targets that are mobile and emit a heat wave (e.g., tanks, armored fight vehicles)—a follow-up control of the orientation of the gyroscope axis based on signals from the head equipped with an infrared detector or (2) for stationary targets (e.g., underground bunkers, bridges)—a program control of the orientation of a gyroscope axis based on exact data about the target's positions. The determination of the TOL corresponds to the solution of the system of differential equations (5.52) and (5.53). Next, an on-board computer calculates the kinematic path of a bomb flight for one of the previously considered cases (target attack at an angle of 0°, 90°, and 180°). The obtained data are transmitted to the bomb's automatic pilot, where control signals are elaborated for actuators of a rudder and an elevator.

In general, the schematic of gyroscopic control of a bomb control automatically moving toward a ground target is presented in Fig. 5.15.

Programmed control moments for the case of tracking of a stationary target (very often a hidden, underground one) are as follows:

$$M_b = M_b^n = J_{gk}\frac{\mathrm{d}^2\vartheta_{gz}}{\mathrm{d}t^2} + \frac{1}{2}J_{gk}\dot{\psi}_{gz}^2\sin 2\vartheta_{gz} + J_{go}n_g\dot{\psi}_{gz}\cos\vartheta_{gz} + \eta_b\dot{\vartheta}_{gz}, \tag{5.69a}$$

$$M_c = M_c^n = J_{gk}\frac{\mathrm{d}^2\psi_{gz}}{\mathrm{d}t^2}\cos^2\vartheta_{gz} - J_{gk}\dot{\psi}_{gz}\dot{\vartheta}_{gz}\sin 2\vartheta_{gz} - J_{go}n_g\dot{\vartheta}_{gz}\cos\vartheta_{gz} + \eta_c\dot{\psi}_{gz}, \tag{5.69b}$$

where $\vartheta_{gz} = \epsilon$, $\psi_{gz} = \sigma$ are the angles defining the required orientation of the gyroscope axis in space.

Quantities ϵ and σ and their first and second time derivatives are determined from relationship (5.52a) and then substituted into (5.69a)

$$\frac{\mathrm{d}^2\varepsilon}{\mathrm{d}t^2} = \frac{r_b\dot{\varepsilon}\dot{\sigma}\sin\sigma - \dot{r}_b\dot{\varepsilon}\cos\sigma}{r_b\cos\sigma}$$
$$+ \frac{V_c\dot{\chi}_c\sin\chi_c\sin(\varepsilon-\gamma_c) - \dot{V}_c\cos\chi_c\sin(\varepsilon-\gamma_c) - V_c(\dot{\varepsilon}-\dot{\gamma}_c)\cos\chi_c\cos(\varepsilon-\gamma_c)}{r_b\cos\sigma}$$
$$+ \frac{V_b\dot{\chi}_b\sin\chi_b\sin(\varepsilon-\gamma_b) - \dot{V}_b\cos\chi_b\sin(\varepsilon-\gamma_b) + V_b(\dot{\varepsilon}-\dot{\gamma}_b)\cos\chi_b\cos(\varepsilon-\gamma_b)}{r_b\cos\sigma},$$

$$\frac{\mathrm{d}^2\sigma}{\mathrm{d}t^2} = -\frac{\dot{r}_b}{r_b}\dot{\sigma} - \frac{\dot{V}_c}{r_b}[\cos(\varepsilon-\gamma_c)\sin\sigma\cos\chi_c - \cos\sigma\sin\chi_c]$$
$$- \frac{V_c}{r_b}[\dot{\chi}_c\sin\chi_c\sin\sigma\cos(\varepsilon-\gamma_c) - \dot{\sigma}\cos\chi_c\cos\sigma\cos(\varepsilon-\gamma_c)$$
$$+ (\dot{\varepsilon}-\dot{\gamma}_c)\cos\chi_c\sin\sigma\sin(\varepsilon-\gamma_c) + \dot{\chi}_c\cos\chi_c\cos\sigma - \dot{\sigma}\sin\chi_c\sin\sigma]$$
$$+ \frac{\dot{V}_b}{r_b}[\cos(\varepsilon-\gamma_b)\sin\sigma\cos\chi_b - \cos\sigma\sin\chi_b]$$
$$- \frac{V_b}{r_b}[\dot{\chi}_b\sin\chi_b\sin\sigma\cos(\varepsilon-\gamma_b) + \dot{\sigma}\cos\chi_b\cos\sigma\cos(\varepsilon-\gamma_b)$$
$$+ (\dot{\varepsilon}-\dot{\gamma}_b)\cos\chi_b\sin\sigma\sin(\varepsilon-\gamma_b) + \dot{\chi}_b\cos\chi_b\cos\sigma - \dot{\sigma}\sin\chi_b\sin\sigma],$$

where

$$\frac{\mathrm{d}^2 r_b}{\mathrm{d}t^2} = \dot{V}_c[\cos(\varepsilon-\gamma_c)\cos\sigma\cos\chi_c + \sin\sigma\sin\chi_c]$$
$$- V_c[\dot{\chi}_c\sin\chi_c\cos\sigma\cos(\varepsilon-\gamma_c) + \dot{\sigma}\cos\chi_c\sin\sigma\cos(\varepsilon-\gamma_c)$$
$$+ (\dot{\varepsilon}-\dot{\gamma}_c)\cos\chi_c\cos\sigma\sin(\varepsilon-\gamma_c) - \dot{\chi}_c\cos\chi_c\sin\sigma - \dot{\sigma}\sin\chi_c\cos\sigma]$$
$$- V_b[\cos(\varepsilon-\gamma_b)\cos\sigma\cos\chi_b + \sin\sigma\sin\chi_b]$$
$$- \dot{V}_b[\cos(\varepsilon-\gamma_b)\cos\sigma\cos\chi_b + \sin\sigma\sin\chi_b]$$
$$- V_b[\dot{\chi}_b\sin\chi_b\cos\sigma\cos(\varepsilon-\gamma_b) + \dot{\sigma}\cos\chi_b\sin\sigma\cos(\varepsilon-\gamma_b)$$
$$+ (\dot{\varepsilon}-\dot{\gamma}_b)\cos\chi_b\cos\sigma\sin(\varepsilon-\gamma_b) - \dot{\chi}_b\cos\chi_b\sin\sigma - \dot{\sigma}\sin\chi_b\cos\sigma].$$

In the case where $V_c = 0$ (a stationary target), we have

$$\vartheta_{gz} = \varepsilon, \qquad \psi_{gz} = \sigma, \tag{5.70}$$

$$\frac{\mathrm{d}\vartheta_{gz}}{\mathrm{d}t} = \frac{\mathrm{d}\varepsilon}{\mathrm{d}t} = \frac{V_b\sin(\varepsilon-\gamma_b)\cos\chi_b}{r\cos\sigma}, \tag{5.71}$$

$$\frac{\mathrm{d}\psi_{gz}}{\mathrm{d}t} = \frac{\mathrm{d}\sigma}{\mathrm{d}t} = V_b \frac{\cos(\varepsilon - \gamma_b)\sin\sigma\cos\chi_b - \cos\sigma\sin\chi_b}{r}, \tag{5.72}$$

$$\frac{\mathrm{d}^2\vartheta_{gz}}{\mathrm{d}t^2} = \frac{\mathrm{d}^2\varepsilon}{\mathrm{d}t^2} = \frac{\sin(\varepsilon - \gamma_b)\cos\chi_b}{r\cos\sigma}\left(\frac{\mathrm{d}V_b}{\mathrm{d}t} - V_b\frac{\frac{\mathrm{d}r}{\mathrm{d}t}\cos\sigma - r\frac{\mathrm{d}\sigma}{\mathrm{d}t}\sin\sigma}{r\cos\sigma}\right)$$
$$+V_b\frac{\left(\frac{\mathrm{d}\varepsilon}{\mathrm{d}t} - \frac{\mathrm{d}\gamma_b}{\mathrm{d}t}\right)\cos(\varepsilon - \gamma_b) - \frac{\mathrm{d}\chi_b}{\mathrm{d}t}\sin(\varepsilon - \gamma_b)\sin\chi_b}{r\cos\sigma}, \tag{5.73}$$

$$\frac{\mathrm{d}^2\psi_{gz}}{\mathrm{d}t^2} = \frac{\mathrm{d}^2\sigma}{\mathrm{d}t^2} = \frac{\cos(\varepsilon - \gamma_b)\sin\sigma\cos\chi_b - \cos\sigma\sin\chi_b}{r}\left(\frac{\mathrm{d}V_b}{\mathrm{d}t} - \frac{V_b}{r}\frac{\mathrm{d}r}{\mathrm{d}t}\right)$$
$$+\frac{V_b}{r}\left[\left(\frac{\mathrm{d}\gamma_b}{\mathrm{d}t} - \frac{\mathrm{d}\varepsilon}{\mathrm{d}t}\right)\sin(\varepsilon - \gamma_b)\sin\sigma\cos\chi_b + \frac{\mathrm{d}\sigma}{\mathrm{d}t}\sin\sigma\sin\chi_b - \frac{\mathrm{d}\chi_b}{\mathrm{d}t}\cos\sigma\cos\chi_b\right]$$
$$+\cos(\varepsilon - \gamma_b)\left(\frac{\mathrm{d}\sigma}{\mathrm{d}t}\cos\sigma\cos\chi_b - \frac{\mathrm{d}\chi_b}{\mathrm{d}t}\sin\sigma\sin\chi_b\right). \tag{5.74}$$

As a result of the influence of all kinds of external disturbances on a gyroscope, the gyroscope axis can perform a prescribed motion with certain unacceptable errors. In this case one should additionally apply correcting control moments M_b^k and M_c^k, which can be represented in the following way:

$$M_b^k = k_b\left(\vartheta_g - \varepsilon\right) - k_c\left(\psi_g - \sigma\right) + h_g\left(\frac{\mathrm{d}\vartheta_g}{\mathrm{d}t} - \frac{\mathrm{d}\varepsilon}{\mathrm{d}t}\right), \tag{5.75a}$$

$$M_c^k = k_b\left(\psi_g - \sigma\right) - k_c\left(\vartheta_g - \varepsilon\right) + h_g\left(\frac{\mathrm{d}\psi_g}{\mathrm{d}t} - \frac{\mathrm{d}\sigma}{\mathrm{d}t}\right), \tag{5.75b}$$

where k_b, k_c, h_g are the gain coefficients of the system of automatic control of a gyroscope.

5.2.4 Control Law for Automatic Pilot of a Guided Bomb

The steering of the flight of a guided bomb is accomplished by means of displacement of control surfaces of ailerons, a rudder, and an elevator respectively by the angles δ_l, δ_m, and δ_n. However, the change in the bomb's flight path is influenced only by the rudder and elevator, which means that we should limit ourselves to determining a control rule for the change in displacement of angles δ_m and δ_n.

The realization of the desired flight path of the guided bomb is carried out by the automatic pilot (AP), which elaborates control signals for the actuator system of the control.

Let us write the control rule for the AP, with the dynamics of displacement of control surfaces taken into account, using the following relationships:

$$\frac{\mathrm{d}^2\delta_m}{\mathrm{d}t^2} + h_{mb}\frac{\mathrm{d}\delta_m}{\mathrm{d}t} + k_{mb}\delta_m = k_{m1}\left(\gamma_{br} - \gamma_b\right) + k_{m2}\left(\frac{\mathrm{d}\gamma_{br}}{\mathrm{d}t} - \frac{\mathrm{d}\gamma_b}{\mathrm{d}t}\right) + h_m\left(\frac{\mathrm{d}^2\gamma_{br}}{\mathrm{d}t^2} - \frac{\mathrm{d}^2\gamma_b}{\mathrm{d}t^2}\right), \tag{5.76a}$$

$$\frac{\mathrm{d}^2\delta_n}{\mathrm{d}t^2} + h_{nb}\frac{\mathrm{d}\delta_n}{\mathrm{d}t} + k_{nb}\delta_n = k_{n1}\left(\chi_{br} - \chi_b\right) + k_{n2}\left(\frac{\mathrm{d}\chi_{br}}{\mathrm{d}t} - \frac{\mathrm{d}\chi_b}{\mathrm{d}t}\right) + h_n\left(\frac{\mathrm{d}^2\chi_{br}}{\mathrm{d}t^2} - \frac{\mathrm{d}^2\chi_b}{\mathrm{d}t^2}\right), \tag{5.76b}$$

where γ_{br}, χ_{br} are the actual angles of the bomb's flight; h_{mb}, k_{mb}, h_{nb}, k_{nb} are coefficients of appropriately selected constants of control surface drives; and h_m, k_{mb}, h_n, k_n are coefficients of appropriately selected constants of a PD-type controller in the autopilot of the bomb.

5.2.5 *Results and Final Conclusions*

In order to validate the system operation, a numerical simulation for a "hypothetical" bomb equipped with a self-guidance system was conducted, where the drive was a controlled gyroscope with the following parameters:

$$J_{gk} = 2.5 \cdot 10^{-4}\,\mathrm{kg}\cdot\mathrm{m}^2, \qquad n_g = 600\,\frac{\mathrm{rad}}{\mathrm{s}}, \qquad \eta_b = \eta_c = 0.01\,\frac{\mathrm{N}\cdot\mathrm{m}\cdot\mathrm{s}}{\mathrm{rad}}.$$

Parameters of the gyroscope controller were selected in an optimal way with respect to minimal error between the prescribed and actual motions. The value of the coefficient was taken as

$$k_b = 10\,\frac{\mathrm{N}\cdot\mathrm{m}}{\mathrm{rad}},$$

whereas the remaining ones are determined in the following way [19]:

$$k_c = \frac{1}{2}\frac{J_{go}^2 n_g^2}{J_{gk}}\sqrt{2J_{go}^2 n_g^2 + 4J_{gk}k_b}, \qquad h_g = \sqrt{2J_{go}^2 n_g^2 + 4J_{gk}k_b}.$$

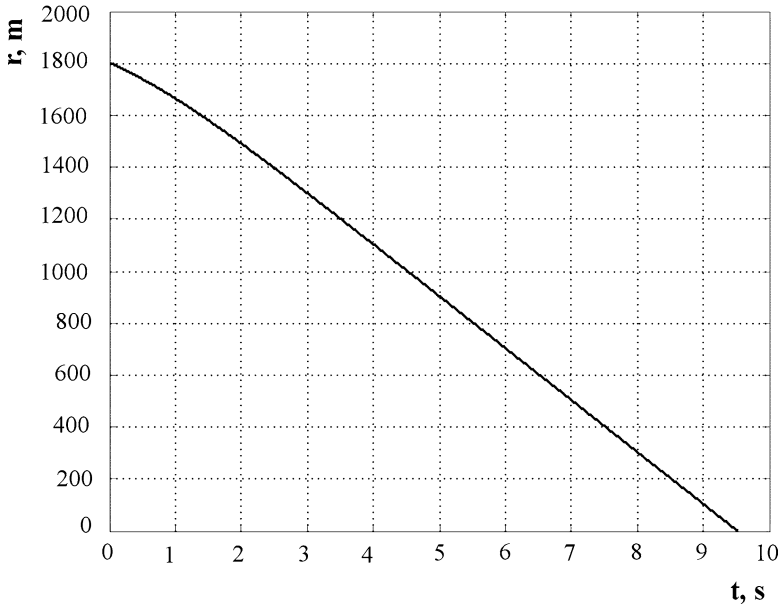

Fig. 5.16 Change in time of relative distance r between bomb and target

The coefficients of gain and damping of the autopilot of the guided bomb are obtained in a similar way:

$$k_{m1} = k_{n1} = 2.703, \qquad k_{m2} = k_{n2} = 11.439, \qquad h_m = h_n = 9.887.$$

Some results of investigations are presented in Figs. 5.16–5.31, where Figs. 5.16–5.19 show the flight trajectories of a bomb guiding itself to a stationary ground target. For comparison we refer to the trajectories for guidance with proportional navigation method (dashed lines) and trajectories for attacks on the aforementioned ground targets at different angles: 90°, 0°, 180° (dashed lines).

It should be emphasized that the TOL in the considered self-guidance system of a bomb is identified with the axis of the controlled gyroscope. An open-loop control system of a gyroscope axis does not function properly (it indicates the target inaccurately), even when there are no external disturbances (Figs. 5.20–5.23). The cause of errors is the friction in the bearings of the gyroscope's suspension. If additionally there appears a disturbance (acting in the time interval $3.0\,\text{s} \leq t \leq 4.5\,\text{s}$), then a large discrepancy occurs between the prescribed and actual (realized) motions of both the axis of the gyroscope (Figs. 5.24 and 5.25) and the flight path of the bomb itself (Figs. 5.26 and 5.27).

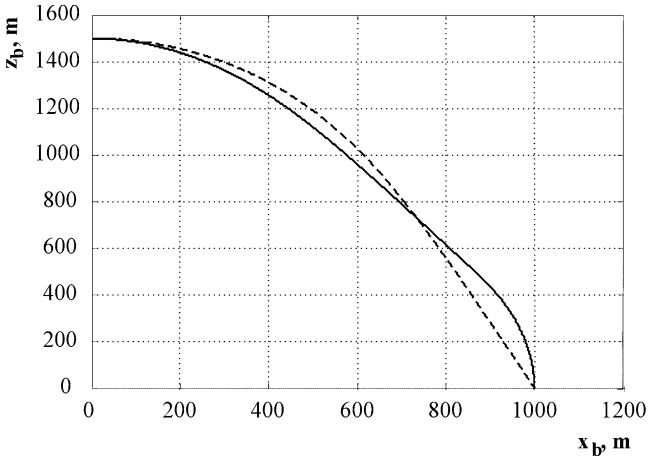

Fig. 5.17 Bomb flight trajectory in accordance with proportional navigation (dashed line) and during attack at an angle of 90° (continuous line)

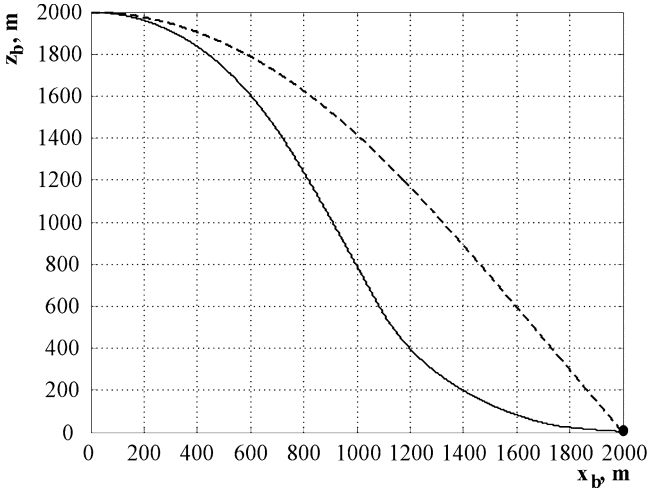

Fig. 5.18 Bomb flight trajectory in accordance with proportional navigation (dashed line) and during attack at an angle of 0° (continuous line)

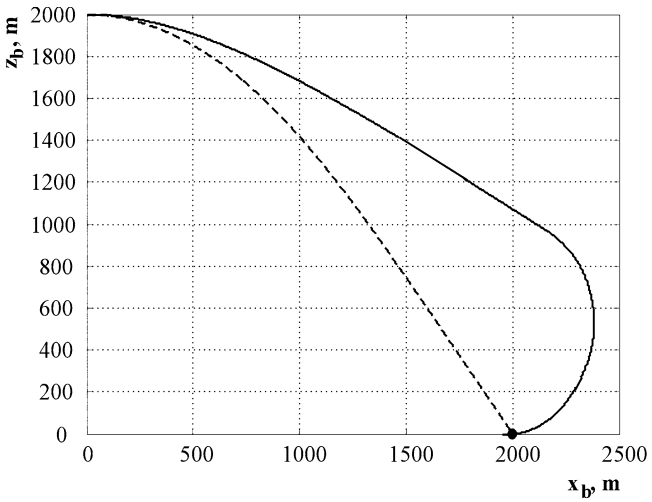

Fig. 5.19 Bomb flight trajectory in accordance with proportional navigation (dashed line) and during attack at an angle of 180° (continuous line)

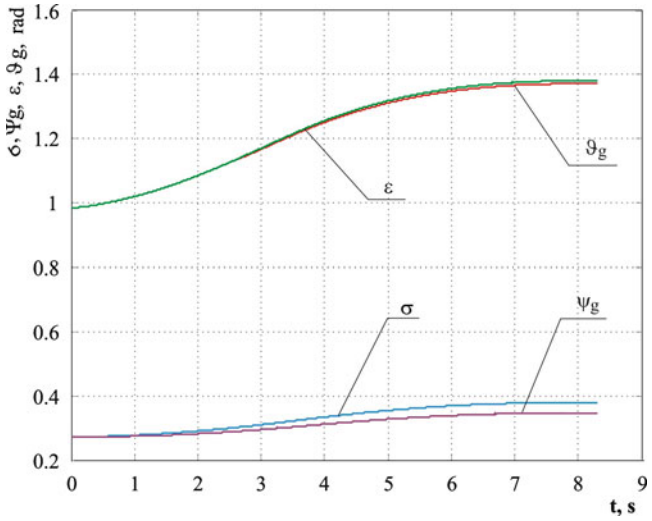

Fig. 5.20 Change in time of angles ϵ, σ of TOL position (prescribed) and angles ϑ_g, Ψ_g of gyroscope axle position, without correcting moments

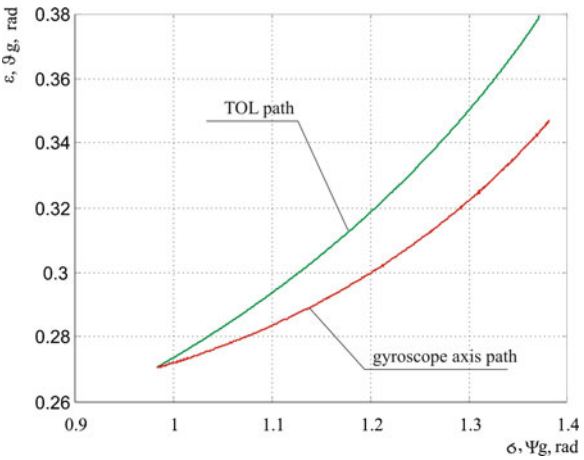

Fig. 5.21 Motion paths of TOL and gyroscope axis, without correcting moments

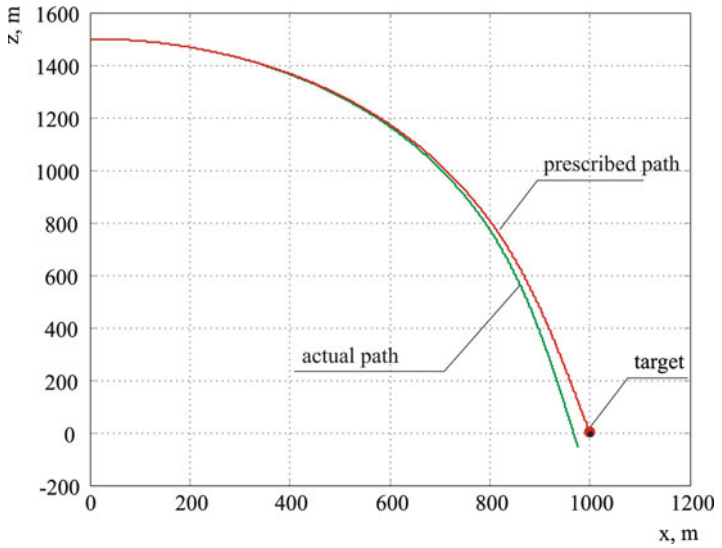

Fig. 5.22 Prescribed and actual paths of bomb flight, without correcting moments

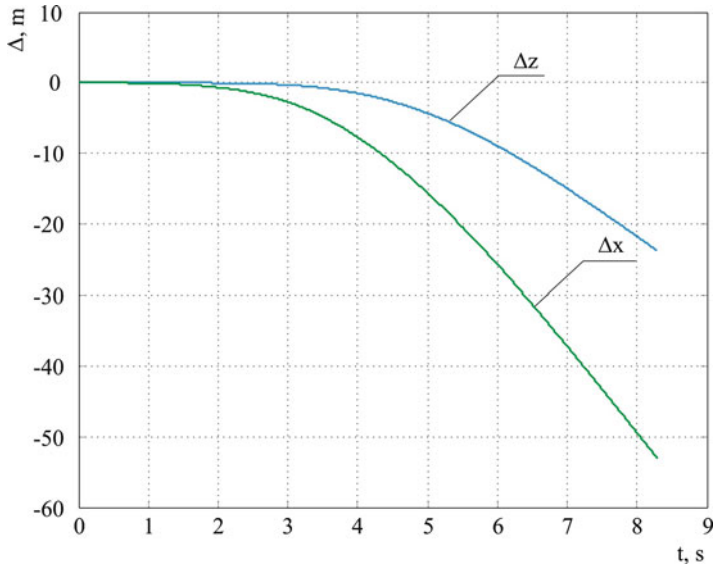

Fig. 5.23 Errors of self-guidance of a bomb without correcting moments

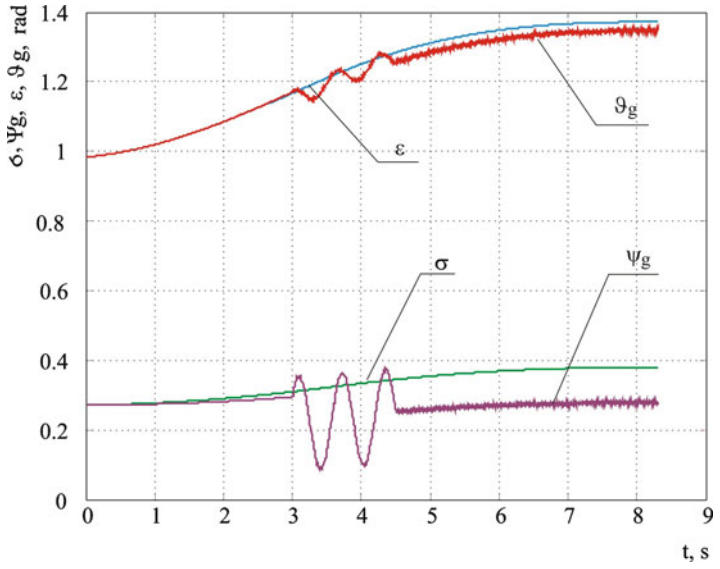

Fig. 5.24 Change in time of angles ϵ, σ of TOL position (prescribed) and angles ϑ_g, ψ_g of gyroscope axis position during appearance of disturbances, without correcting moments

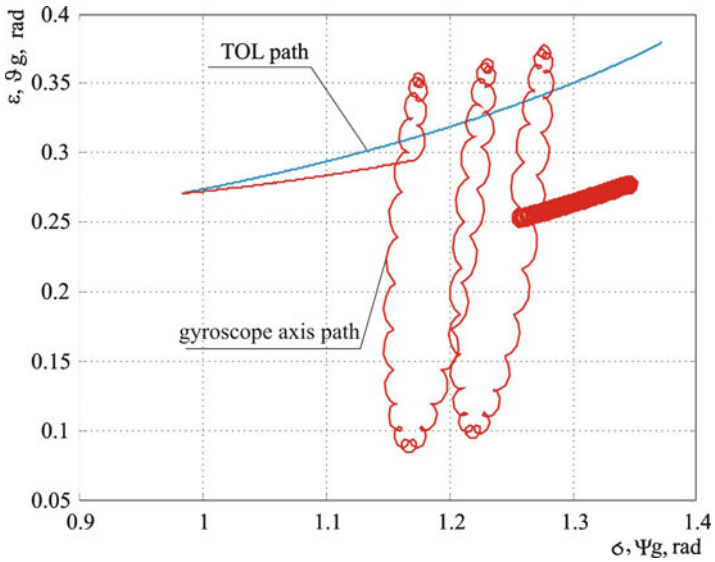

Fig. 5.25 Motion paths of TOL (prescribed) and gyroscope axis (actual) during appearance of disturbance, without correcting moments

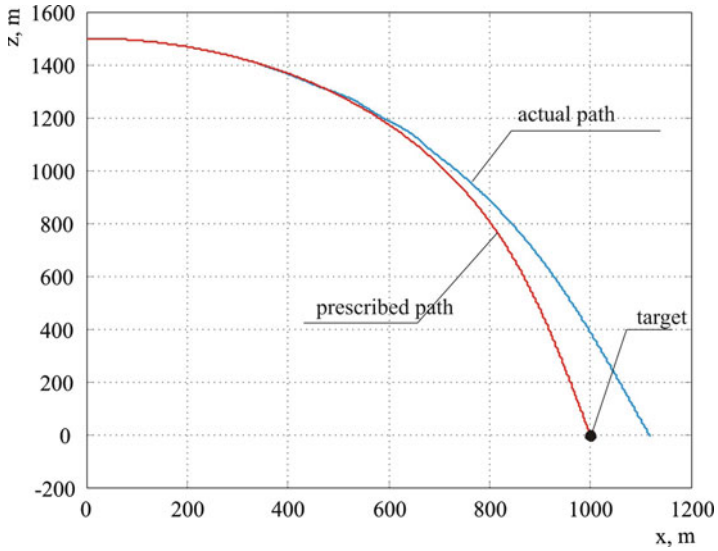

Fig. 5.26 Prescribed and actual flight paths of bomb during appearance of disturbance, without correcting moments

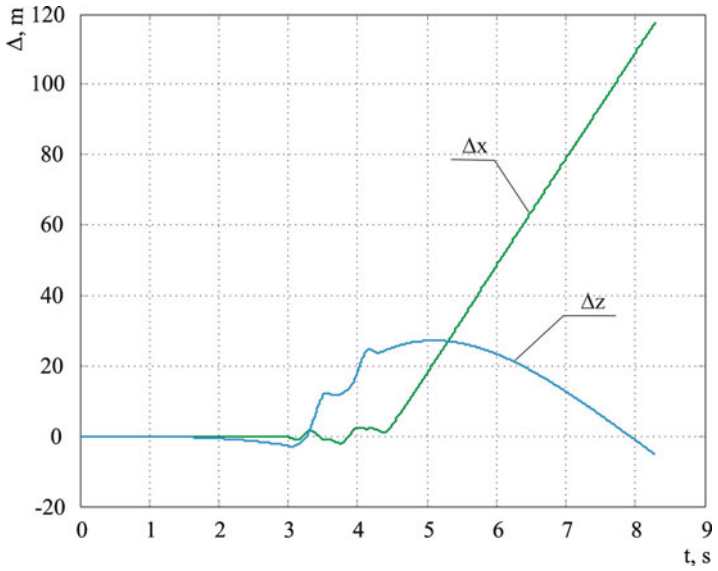

Fig. 5.27 Errors of self-guidance of bomb during appearance of disturbance, without correcting moments

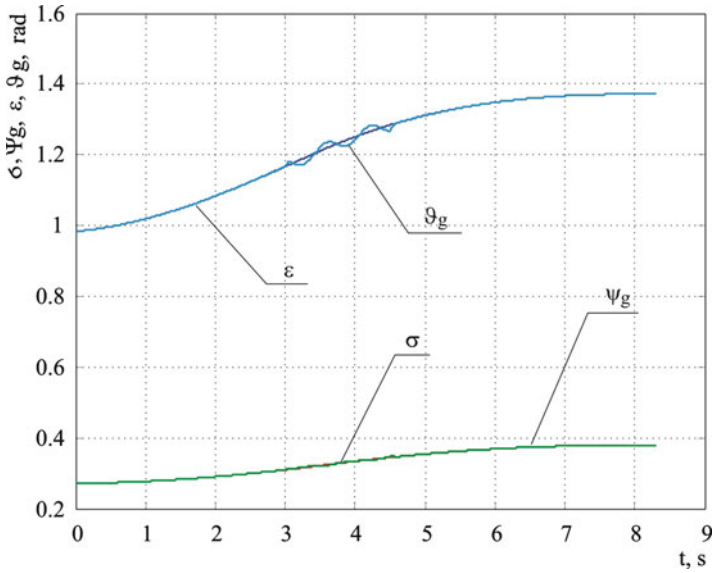

Fig. 5.28 Change in time of angles ϵ, σ of TOL position (prescribed) and angles ϑ_g, ψ_g of gyroscope axis position during appearance of disturbances, with application of correcting moments

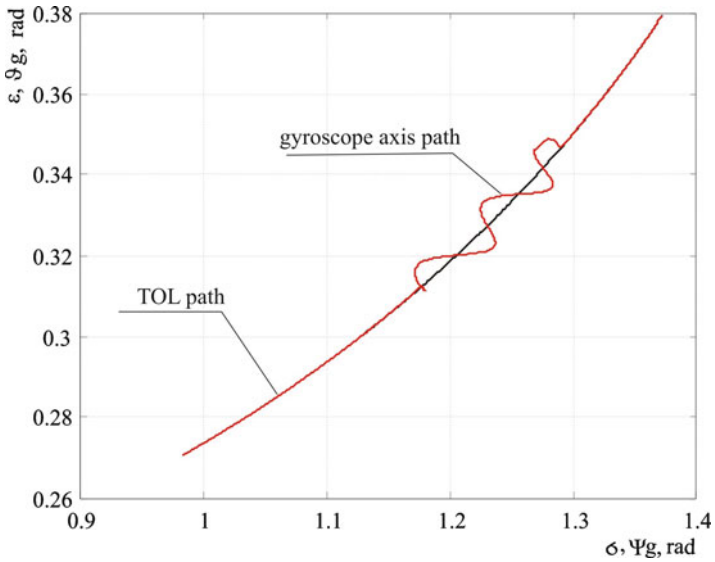

Fig. 5.29 Motion paths of TOL (prescribed) and gyroscope axis (actual) during appearance of disturbance, with application of correcting moments

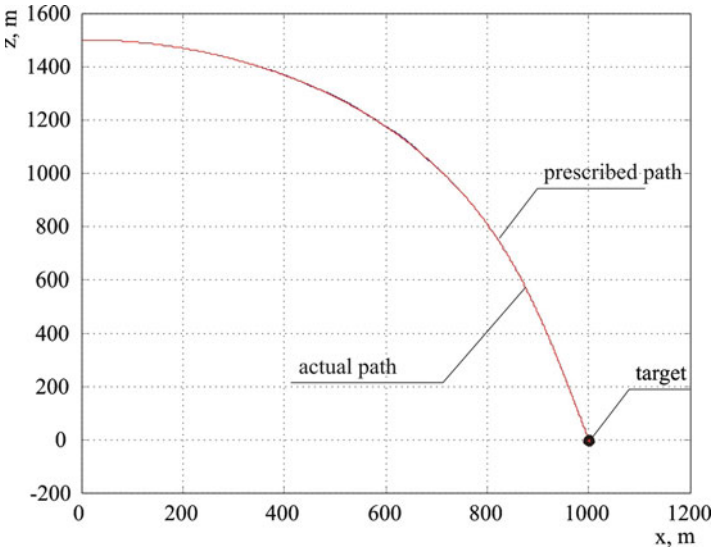

Fig. 5.30 Prescribed and actual flight paths of bomb during appearance of disturbance, with application of correcting moments

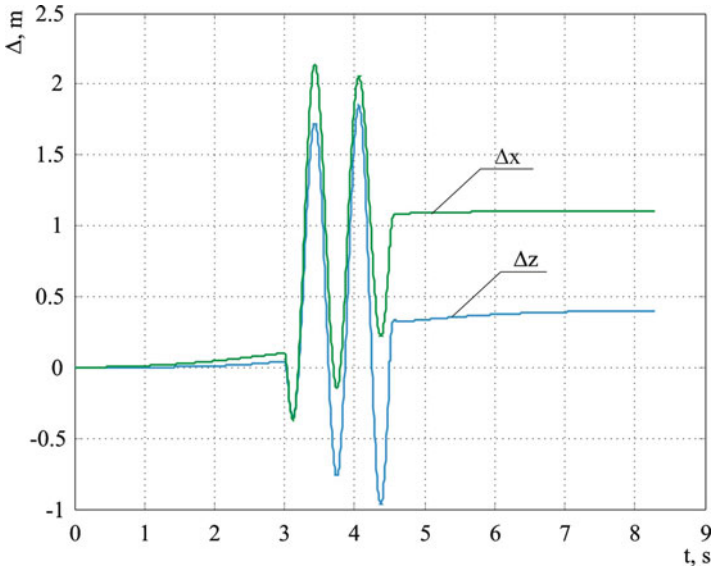

Fig. 5.31 Bomb self-guidance errors during appearance of disturbance, with application of correcting moments

The application of additional feedback in a system of automatic control of motion of the axis of a gyroscope with optimally selected parameters [12] substantially improves the accuracy of the TOL (the alignment of the TOL with the axis of the gyroscope) and consequently the minimization of errors between prescribed and actual motions of both gyroscope and guided bomb. This is clearly illustrated in Figs. 5.28–5.31.

To sum up, it may be stated that preliminary investigations confirm the possibility of application of a gyroscopic system in a guided bomb self-guidance to a ground target. However, in further research the influence of the following factors should be subjected to a more detailed analysis: (a) dry and viscous friction in frame bearings; (b) frame inertia; (c) unbalance (static and dynamic) of a rotor with respect to the intersection of frame axes, that is, the center of rotation; (d) the linear and angular acceleration of the base; (e) the elasticity of structural elements; (f) the errors of a Cardan suspension; (g) the instability of the rotor drive; (h) the intersection of the frames at angles other than 90°; (i) large angles and angular velocities of deviation of the main axis of the gyroscope from the prescribed direction; and (j) the Earth's rotational motion about its axis. Those factors have ultimate influence on the accuracy of the bomb. Moreover, various methods of self-guidance should be investigated with respect to the time to reach targets and the minimization of a gravity load acting on a bomb when approaching a target.

References

1. Z. Koruba, A mathematical model of the dynamics and control of a gyroscopic platform mounted on board of an aerial vehicle. J. Tech. Phys. **46**(1), 37–50 (2005)
2. Z. Koruba, A process of gyroscope motion control in an autonomous system, target detection and tracking. J. Theor. Appl. Mech. **37**(4), 908–927 (1999)
3. Z. Koruba, Adaptive correction of controlled gyroscope on the deck of aerial object. J. Tech. Phys. **42**(2), 203–222 (2001)
4. T.S. Taylor, *Introduction to Rocket Science and Engineering* U.S. Army Space and Missile Defense Command. (Huntsville, AL, 2009)
5. Z. Koruba, Model of final navigation segment for combat unmanned aerial vehicle. J. Tech. Phys. **44**(1), 99–115 (2003)
6. R. Yanushevsky, *Modern Missile Guidance* (CRC Press, Boca Raton, FL, 2007)
7. Z. Koruba, J. Osiecki, *Construction, Dynamics and Navigation of Close-Range Missiles, Part 1*. University Course Book No. 348 (Kielce University of Technology Press, Kielce, 1999), in Polish
8. J.H. Blakelock, *Automatic Control of Aircraft and Missiles* (Wiley, New York, 1991)
9. Z. Koruba, in *The Model of the Control of Aerial Robot with Autonomous System of Ground Object Seeking and Tracking*. Proceedings of the First Workshop on Robot Motion and Control (1999), pp. 41–44
10. Z. Koruba, Unmanned aerial vehicle flight programme, ground surface scanning and laser target illumination. J. Tech. Phys. **40**(4), 421–434 (1999)
11. G.M. Siouris, *Missile Guidance and Control Systems* (Springer, New York, 2004)
12. Z. Koruba, Optimisation of construction parameters of gyroscope system on elastic suspension. Comput. Assist. Mech. Eng. Sci. **4**(7), 595–606 (2000)
13. Z. Koruba, in *Dynamics and control model of gyroscope located on deck unmanned aerial vehicle.* North Atlantic Treaty Organization Unmanned Vehicles for Aerial, Ground and Naval Military Operations – a Symposium organised by the Applied Vehicle Technology Panel, Ankara, Turkey, 9–13 October 2000
14. Z. Koruba, J. Osiecki, *Construction, Dynamics and Navigation of Selected Arms of Precision Strike* (Kielce University of Technology Press, Kielce, 2006), in Polish
15. K. Ogata, *Matlab for Control Engineers* (Prentice-Hall, Engewood Cliffs, NJ, 2007)
16. P. De Larminat, Y. Thomas, *Automatics of Linear Systems*, vol. 3 (Flammarion Sciences, Paris, 1977), in French
17. B. Kisacanin, *Linear Control Systems: with Solved Problems and MATLAB Examples* (Kluwer/Plenum, New York, 2002)
18. Da-Wei Gu, P.H. Petkov, M.M. Konstantinov, *Robust Control Design with MATLAB* (Springer, London, 2005)
19. Z. Koruba, K. Ogonowski, The analysis of a gyroscopic system in the process of guiding an aerial bomb to a water target. Polish J. Environ. Stud. **16**(4A), 92–95 (2007)